A search for top squarks with *R*-parity-violating decays to all-hadronic final states with the ATLAS detector in $\sqrt{s} = 8$ TeV proton–proton collisions

The ATLAS Collaboration

Abstract

A search for the pair production of top squarks, each with *R*-parity-violating decays into two Standard Model quarks, is performed using 17.4 fb^{-1} of $\sqrt{s} = 8$ TeV proton–proton collision data recorded by the ATLAS experiment at the LHC. Each top squark is assumed to decay to a *b*- and an *s*-quark, leading to four quarks in the final state. Background discrimination is achieved with the use of *b*-tagging and selections on the mass and substructure of large-radius jets, providing sensitivity to top squark masses as low as 100 GeV. No evidence of an excess beyond the Standard Model background prediction is observed and top squarks decaying to $\bar{b}\bar{s}$ are excluded for top squark masses in the range $100 \leq m_{\tilde{t}} \leq 315$ GeV at 95% confidence level.

arXiv:1601.07453v3 [hep-ex] 22 Jun 2016

1 Introduction

Supersymmetry (SUSY) is an extension of the Standard Model (SM) [1–7] that fundamentally relates fermions and bosons. It is an especially alluring theoretical possibility given its potential to solve the hierarchy problem [8–11] and to provide a dark-matter candidate [12, 13].

This paper presents a search for the pair production of supersymmetric top squarks (stops)[1], which then each decay to two SM quarks, using 17.4 fb^{-1} of $\sqrt{s} = 8$ TeV proton–proton (pp) collision data recorded by the ATLAS experiment at the Large Hadron Collider (LHC). This decay violates the R-parity conservation (RPC) [14] assumed by most searches for stops [15, 16]. In RPC scenarios, SUSY particles are required to be produced in pairs and decay to the lightest supersymmetric particle (LSP), which is stable. In R-parity-violating (RPV) models, decays to only SM particles are allowed, and generally relax the strong constraints now placed on standard RPC SUSY scenarios by the LHC experiments. It is therefore crucial to expand the scope of the SUSY search programme to include RPV models. Common signatures used for RPV searches include resonant lepton-pair production [17], exotic decays of long-lived particles with displaced vertices [18–21], high lepton multiplicities [22, 23], and high-jet-multiplicity final states [24]. Scenarios which have stops of mass below 1 TeV are of particular interest as these address the hierarchy problem [25–28].

SUSY RPV decays to SM quarks and leptons are controlled by three Yukawa couplings in the generic supersymmetric superpotential [29, 30]. These couplings are represented by $\lambda_{ijk}, \lambda'_{ijk}, \lambda''_{ijk}$, where $i, j, k \in$ $1, 2, 3$ are generation indices that are sometimes omitted in the discussion that follows. The first two (λ, λ') are lepton-number-violating couplings, whereas the third (λ'') violates baryon number. It is therefore generally necessary that either of the couplings to quarks, λ' or λ'', be vanishingly small to prevent spontaneous proton decay [7]. It is common to consider non-zero values of each coupling separately. Scenarios in which $\lambda'' \neq 0$ are often referred to UDD scenarios because of the baryon-number-violating term that λ'' controls in the superpotential. Current indirect experimental constraints [31] on the sizes of each of the UDD couplings λ'' from sources other than proton decay are primarily valid for low squark mass and for first- and second-generation couplings. Those limits are driven by double nucleon decay [32] (for λ''_{112}), neutron oscillations [33] (for λ''_{113}), and Z-boson branching ratios [34].

The benchmark model considered in this paper is a baryon-number-violating RPV scenario in which the stop is the LSP. The search specifically targets low-mass stops in the range 100–400 GeV that decay via the λ''_{323} coupling, thus resulting in stop decays $\tilde{t} \to \bar{b}\bar{s}$ (assuming a 100% branching ratio) as shown in Figure 1. The motivation to focus on the third-generation UDD coupling originates primarily from the minimal flavour violation (MFV) hypothesis [35] and the potential for this decay channel to yield a possible signal of RPV SUSY with a viable dark-matter candidate [36]. The MFV hypothesis essentially requires that all flavour- and CP-violating interactions are linked to the known structure of Yukawa couplings, and has been used to argue for the importance of the λ'' couplings [37].

The process $\tilde{t}\tilde{t}^* \to \bar{b}\bar{s}bs$ represents an important channel in which to search for SUSY in scenarios not yet excluded by LHC data [36–38]. Some of the best constraints on this process are from the ALEPH Collaboration, which set lower bounds on the mass of the stop at $m_{\tilde{t}} \gtrsim 80$ GeV [39]. The CDF Collaboration extended these limits, excluding $50 \lesssim m_{\tilde{t}} \lesssim 90$ GeV [40]. The CMS Collaboration recently released the results of a search that excludes $200 \lesssim m_{\tilde{t}} \lesssim 385$ GeV [41] in the case where heavy-flavour jets are present in the final state. In addition, two ATLAS searches have placed constraints on RPV stops that

---

[1] The superpartners of the left- and right-handed top quarks, $\tilde{t}_{\mathrm{L}}$ and $\tilde{t}_{\mathrm{R}}$, mix to form the two mass eigenstates $\tilde{t}_1$ and $\tilde{t}_2$, where $\tilde{t}_1$ is the lighter one. This analysis focuses on $\tilde{t}_1$, which is referred to hereafter as $\tilde{t}$.

decay to $\bar{b}\bar{s}$ when they are produced in the decays of light gluinos ($m_{\tilde{g}} \lesssim 900$–1000 GeV) [42, 43]. The search presented here specifically focuses on direct stop pair production and seeks to close the gap in excluded stop mass between ~ 100–200 GeV. Contributions from RPV interactions at production – such as would be required for resonant single stop production – are neglected in this analysis. This approach is valid provided that the RPV interaction strength is small compared to the strong coupling constant, which is the case for $\lambda''_{323} \lesssim 10^{-2}$–$10^{-1}$ [44] and for the estimated size of $\lambda''_{323} \sim 10^{-4}$ from MFV in the model described in Ref. [37].

The reduced sensitivity of standard SUSY searches to RPV scenarios is primarily due to the limited effectiveness of the high missing transverse momentum requirements used in the event selection common to many of those searches, motivated by the assumed presence of undetected LSPs. Consequently, the primary challenge in searches for RPV SUSY final states is to identify suitable substitutes for background rejection to the canonical large missing transverse momentum signature.
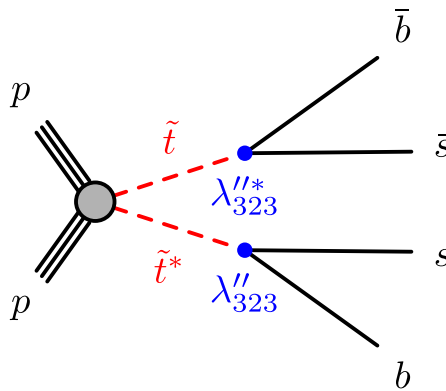

Figure 1: Benchmark signal process considered in this analysis. The solid black lines represent Standard Model particles, the dashed red lines represent the stops, and the blue points represent RPV vertices labelled by the relevant coupling for this diagram.

Backgrounds dominated by multijet final states typically overwhelm the signal in the four-jet topology. In order to overcome this challenge, new observables are employed to search for $\tilde{t}\tilde{t}^* \to \bar{b}\bar{s}bs$ in the low-$m_{\tilde{t}}$ regime [38]. For $m_{\tilde{t}} \approx 100$–300 GeV, the initial stop transverse momentum (p_T) spectrum extends significantly into the range for which $p_T \gg m_{\tilde{t}}$. This feature is the result of boosts received from initial-state radiation (ISR) as well as originating from the parton distribution functions (PDFs). As the Lorentz boost of each stop becomes large, the stop decay products begin to merge with a radius roughly given by $\Delta R \approx 2m_{\tilde{t}}/p_T$, and thus can be clustered together within a single large-radius (large-R) jet with a mass $m^{\text{jet}} \approx m_{\tilde{t}}$. By focusing on such cases, the dijet and multijet background can be significantly reduced via selections that exploit this kinematic relationship and the structure of the resulting *stop jet*, in a similar way to boosted objects used in previous measurements and searches by ATLAS [45–49]. In this case, since the stop is directly produced in pairs instead of from the decay of a massive parent particle, the strategy is most effective at low $m_{\tilde{t}}$ where the boosts are the largest.

2 The ATLAS detector

The ATLAS detector [50,51] provides nearly full solid angle[2] coverage around the collision point with an inner tracking system (inner detector, or ID) covering the pseudorapidity range $|\eta| < 2.5$, electromagnetic (EM) and hadronic calorimeters covering $|\eta| < 4.9$, and a muon spectrometer covering $|\eta| < 2.7$ that provides muon trigger capability up to $|\eta| < 2.4$.

The ID comprises a silicon pixel tracker closest to the beamline, a microstrip silicon tracker, and a straw-tube transition-radiation tracker at radii up to 108 cm. A thin solenoid surrounding the tracker provides a 2 T axial magnetic field enabling the measurement of charged-particle momenta. The overall ID acceptance spans the full azimuthal range in ϕ, and the range $|\eta| < 2.5$ for particles originating near the nominal LHC interaction region [52].

The EM and hadronic calorimeters are composed of multiple subdetectors spanning $|\eta| \leq 4.9$. The EM barrel calorimeter uses a liquid-argon (LAr) active medium and lead absorbers. In the region $|\eta| < 1.7$, the hadronic (Tile) calorimeter is constructed from steel absorber and scintillator tiles and is separated into barrel ($|\eta| < 1.0$) and extended-barrel ($0.8 < |\eta| < 1.7$) sections. The endcap ($1.375 < |\eta| < 3.2$) and forward ($3.1 < |\eta| < 4.9$) regions are instrumented with LAr calorimeters for EM as well as hadronic energy measurements.

A three-level trigger system is used to select events to record for offline analysis. The different parts of the trigger system are referred to as the level-1 trigger, the level-2 trigger, and the event filter [53]. The level-1 trigger is implemented in hardware and uses a subset of detector information to reduce the event rate to a design value of at most 75 kHz. The level-1 trigger is followed by two software-based triggers, the level-2 trigger and the event filter, which together reduce the event rate to a few hundred Hz. The search presented in this document uses a trigger that requires a high-p_T jet and a large summed jet transverse momentum (H_T), as described in Section 5.

3 Monte Carlo simulation samples

Monte Carlo (MC) simulation is used to study the signal acceptance and systematic uncertainties, to test the background estimation methods used, and to estimate the $t\bar{t}$ background. In all cases, events are passed through the full GEANT4 [54] detector simulation of ATLAS [55] after the simulation of the parton shower and hadronisation processes. Following the detector simulation, identical event reconstruction and selection criteria are applied to both the MC simulation and to the data. Multiple pp collisions in the same and neighbouring bunch crossings (pile-up) are simulated for all samples by overlaying additional soft pp collisions which are generated with PYTHIA 8.160 [56] using the ATLAS A2 set of tuned parameters (tune) in the MC generator [57] and the MSTW2008LO PDF set [58]. These additional interactions are overlaid onto the hard scatter and events are reweighted such that the MC distribution of the average number of pp interactions per bunch crossing matches the measured distribution in the full 8 TeV data sample.

---

[2] The ATLAS reference system is a Cartesian right-handed coordinate system, with the nominal collision point at the origin. The anticlockwise beam direction defines the positive z-axis, while the positive x-axis is defined as pointing from the collision point to the centre of the LHC ring and the positive y-axis points upwards. The azimuthal angle ϕ is measured around the beam axis, and the polar angle θ is measured with respect to the z-axis. Pseudorapidity is defined as $\eta = -\ln[\tan(\theta/2)]$, rapidity is defined as $y = 0.5 \ln[(E + p_z)/(E - p_z)]$, where E is the energy and p_z is the z-component of the momentum, and transverse energy is defined as $E_T = E \sin\theta$.

The signal process is simulated using Herwig++ 2.6.3a [59] with the UEEE3 tune [60] for several stop-mass hypotheses using the PDF set CTEQ6L1 [61, 62]. All non-SM particles masses are set to 5 TeV except for the stop mass, which is scanned in 25 GeV steps from $m_{\tilde{t}} = 100$ GeV to $m_{\tilde{t}} = 400$ GeV.

The signal cross-section used (shown in Figure 2) is calculated to next-to-leading order in the strong coupling constant, adding the resummation of soft gluon emission at next-to-leading-logarithmic accuracy (NLO+NLL) [63–65]. For the range of stop masses considered, the uncertainty on the cross-section is approximately 15% [66]. MadGraph 5.1.4.8 [67] is used to study the impact of ISR on the stop p_{T} spectrum. The MadGraph samples have one additional parton in the matrix element, which improves the modelling of a hard ISR jet. MadGraph is then interfaced to PYTHIA 6.426 with the AUET2B tune [68] and the CTEQ6L1 PDF set for parton shower and hadronisation. The distribution of $p_{\mathrm{T}}(\tilde{t}\tilde{t}^*)$ from the nominal Herwig++ signal sample is then reweighted to match that of the MadGraph+PYTHIA sample.

Dijet and multijet events, as well as top quark pair ($t\bar{t}$) production processes, are simulated in order to study the SM contributions and background estimation techniques. For optimisation studies, SM dijet and multijet events are generated using Herwig++ 2.6.3a with the CTEQ6L1 PDF set. Top quark pair events are generated with the POWHEG-BOX-r2129 [69–71] event generator with the CT10 NLO PDF set [72]. These events are then interfaced to PYTHIA 6.426 with the P2011C tune [73] and the same CTEQ6L1 PDF set as Herwig++.

The $t\bar{t}$ production cross-section is calculated at next-to-next-to-leading order (NNLO) in QCD including resummation of next-to-next-to-leading logarithmic (NNLL) soft gluon terms with top++2.0 [74–79]. The value of the $t\bar{t}$ cross-section is $\sigma_{t\bar{t}} = 253^{+13}_{-15}$ pb.
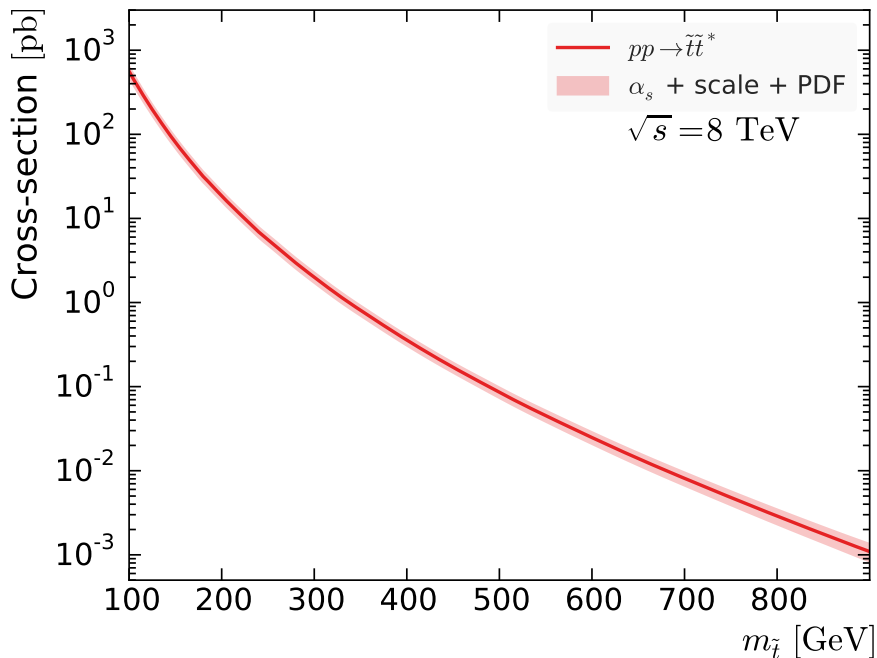
Figure 2: Cross-section for direct $\tilde{t}\tilde{t}^*$ pair production at the LHC centre-of-mass energy of $\sqrt{s} = 8$ TeV [63–65].

4 Object definitions

The data are required to have satisfied criteria designed to reject events with significant contamination from detector noise, non-collision beam backgrounds, cosmic rays, and other spurious effects. To reject non-collision beam backgrounds and cosmic rays, events are required to contain a primary vertex consistent with the LHC beamspot, reconstructed from at least two tracks with transverse momenta $p_T^{track} > 400$ MeV. If more than one vertex satisfies these criteria, the primary vertex is chosen as the one with the highest $\sum_{tracks}(p_T^2)$.

The anti-k_t algorithm [80], with a radius parameter of $R = 0.4$, is used for initial jet-finding using version 3 of FastJet [81]. The inputs to the jet reconstruction are three-dimensional topo-clusters [82]. This method first clusters together topologically connected calorimeter cells and classifies these clusters as either electromagnetic or hadronic. The classification uses a local cluster weighting calibration scheme based on cell-energy density and shower depth within the calorimeter [83]. Based on this classification, energy corrections are applied which are derived from single-pion MC simulations. Dedicated hadronic corrections are derived to account for the effects of differences in response to hadrons compared to electrons, signal losses due to noise-suppression threshold effects, and energy lost in non-instrumented regions. The final jet energy calibration is derived from MC simulation as a correction relating the calorimeter response to the jet energy at generator level. In order to determine these corrections, the same jet definition used in the reconstruction is applied to stable (with lifetimes greater than 10 ps) generator-level particles, excluding muons and neutrinos. A subtraction procedure is also applied in order to mitigate the effects of pile-up [84]. Finally, the $R = 0.4$ jets are further calibrated with additional correction factors derived *in situ* from a combination of γ+jet, Z+jet, and dijet-balance methods [83].

All jets reconstructed with the anti-k_t algorithm using a radius parameter of $R = 0.4$ and a measured $p_T^{jet} > 20$ GeV are required to satisfy the quality criteria discussed in detail in Ref. [85]. These quality criteria selections for jets are extended to prevent contamination from detector noise through several detector-region-specific requirements. Jets contaminated by energy deposits due to noise in the forward hadronic endcap calorimeter are rejected and jets in the central region ($|\eta| < 2.0$) that are at least 95% contained within the EM calorimeter are required to not exhibit any electronic pulse shape anomalies [86]. Any event with a jet that fails these requirements is removed from the analysis.

Identification of jets containing b-hadrons (so-called b-jets) is achieved through the use of a multivariate b-tagging algorithm referred to as MV1 [87]. This algorithm is based on an artificial neural-network algorithm that exploits the impact parameters of charged-particle tracks, the parameters of reconstructed secondary vertices, and the topology of b- and c-hadron decays inside an anti-k_t $R = 0.4$ jet. A working point corresponding to a 70% b-jet efficiency in simulated $t\bar{t}$ events is used. The corresponding mistag rates, defined as the fraction of jets originating from non-b-jets which are tagged by the b-tagging algorithm in an inclusive jet sample, for light jets and c-jets are approximately 1% and 20%, respectively. To account for differences with respect to data, data-derived corrections are applied to the MC simulation for the identification efficiency of b-jets and the probability to mis-identify jets resulting from light-flavour quarks, charm quarks, and gluons.

Initial jet-finding is extended using an approach called *jet re-clustering* [88]. This allows the use of larger-radius jet algorithms while maintaining the calibrations and systematic uncertainties associated with the input jet definition. Small-radius anti-k_t $R = 0.4$ jets with $p_T > 20$ GeV and $|\eta| < 2.4$ are used as input without modification to an anti-k_t $R = 1.5$ large-R jet algorithm, to identify the hadronic stop decays. The small-R jets with $p_T < 50$ GeV are required to have a jet vertex fraction (JVF) of at least 50%. After

summing the p_T of charged-particle tracks matched to a jet, the JVF is the fraction due to tracks from the selected hard-scattering interaction and it provides a means by which to suppress jets from pile-up.

To further improve the background rejection, a splitting procedure is performed on each of the two leading large-R jets. After jet-finding, the constituents of these large-R jets – the anti-k_t R = 0.4 input objects – are processed separately by the Cambridge–Aachen (C/A) algorithm [89, 90], as implemented in FastJet 3. The C/A algorithm performs pair-wise recombinations of proto-jets (the inputs to the jet algorithm) purely based on their angular separation. Smaller-angle pairs are recombined first, thus the final recombined pair typically has the largest separation. The C/A final clustering is then undone by one step, such that there are two branches "a" and "b". The following *splitting* criteria are then applied to the branches "a" and "b" of each of the two leading large-R jets:

- Both branches carry appreciable p_T relative to the large-R jet:

$$\frac{\min[p_T(a), p_T(b)]}{p_T(\text{large}-R)} > 0.1. \tag{1}$$

- The mass of each branch is small relative to its p_T:

$$\frac{m(a)}{p_T(a)} < 0.3 \quad \text{and} \quad \frac{m(b)}{p_T(b)} < 0.3. \tag{2}$$

If either of the leading two large-R jets fails these selections, the event is discarded. This implementation is identical to Ref. [38], which is derived from the diboson-jet tagger [91]. This approach differs somewhat from that used in Ref. [92] in that no requirement is placed on the relative masses of the large-R and small-R jets.

5 Trigger and offline event selections

Events must satisfy jet and H_T selections applied in the trigger which require $H_T = \sum p_T > 500$ GeV, calculated as the sum of level-2 trigger jets within $|\eta| < 3.2$, and a leading jet within $|\eta| < 3.2$ with $p_T > 145$ GeV. This relatively low-threshold jet trigger came online part-way through the data-taking period in 2012 and collected 17.4 fb^{-1} of data. The corresponding offline selections require events to have at least one anti-k_t R = 0.4 jet with $p_T > 175$ GeV and $|\eta| < 2.4$, as well as $H_T > 650$ GeV, where the sum is over all anti-k_t R = 0.4 jets with $p_T > 20$ GeV, $|\eta| < 2.4$, and JVF > 0.5 if $p_T < 50$ GeV. The cumulative trigger selection efficiency is greater than 99% for these offline requirements. The offline event preselection further requires that at least two large-R jets with $p_T > 200$ GeV and mass > 20 GeV be present in each event. These requirements select a range of phase space for low stop masses in which the transverse momentum of the stops is often significantly greater than their mass.

The signal region (SR) is defined to suppress the large multijet background and to enhance the fraction of events that contain large-R jets consistent with the production of stop pairs, with each stop decaying to a light quark and a b-quark. Simulation studies indicate that three kinematic observables are particularly useful for background discrimination:

7

1. The mass asymmetry between the two leading large-R jets in the event (with masses m_1 and m_2, respectively), defined as

$$\mathcal{A} = \frac{|m_1 - m_2|}{m_1 + m_2},\qquad(3)$$

differentiates signal from background since the two stop subjet-pair resonances are expected to be of equal mass.

2. The (absolute value of the cosine of the) stop-pair production angle, $|\cos\theta^*|$, with respect to the beam line in the centre-of-mass reference frame[3] distinguishes between centrally produced massive particles and high-mass forward-scattering events from QCD. It provides efficient discrimination and does not exhibit significant variation with the stop mass.

3. In addition, a requirement on the subjets is applied to each of the leading large-R jets in the event. The p_T of each subjet a and b relative to the other is referred to as the subjet p_{T2}/p_{T1}, defined by

$$\text{subjet } p_{T2}/p_{T1} = \frac{\min[p_T(a), p_T(b)]}{\max[p_T(a), p_T(b)]}.\qquad(4)$$

The $\mathcal{A}$, $|\cos\theta^*|$, and subjet p_{T2}/p_{T1} variables provide good discrimination between signal and background and are motivated by an ATLAS search for scalar gluons at $\sqrt{s} = 7$ TeV [93] as well as by Refs. [38,94].

In addition to the kinematic observables described above, b-tagging applied to anti-k_t $R = 0.4$ jets provides a very powerful discriminant for defining both the signal and the control regions, and one that is approximately uncorrelated with the kinematic features discussed above. Using these kinematic observables and the presence of at least two b-tagged jets per event, the signal region is defined by (for the leading two large-R jets)

$$\begin{aligned}
\mathcal{A} &< 0.1, \\
|\cos\theta^*| &< 0.3, \qquad(5)\\
\text{subjet } p_{T2}/p_{T1} &> 0.3.
\end{aligned}$$

Distributions of the discriminating variables are shown in Figure 3. Insofar as the data points are dominated by background in these plots, even in the case of a potential signal, the data points should be understood to represent the background.

Following these selections, the distribution of the average mass of the leading two large-R jets, $m_{\text{avg}}^{\text{jet}} = (m_1^{\text{jet}} + m_2^{\text{jet}})/2$, is used to search for an excess of events above the background prediction. The search is done in regions of $m_{\text{avg}}^{\text{jet}}$ that are optimised to give the best significance. As shown in Figure 4, the stop signal is expected as a peak that would appear on top of a smoothly falling background spectrum. A Gaussian distribution is fitted to the stop signal $m_{\text{avg}}^{\text{jet}}$ peak. The mean of the fit, $\langle m_{\text{avg}}^{\text{jet}} \rangle$, is consistent with $m_{\tilde{t}}$ in each case. The resolution of the $m_{\text{avg}}^{\text{jet}}$ peak is given approximately $s/\langle m_{\text{avg}}^{\text{jet}} \rangle \sim 5-7\%$ (where s is the standard deviation of the fit), and has only a weak dependence on the stop mass in the range probed by this analysis. Mass *windows* in $m_{\text{avg}}^{\text{jet}}$ are determined by taking into account the effect of jet energy scale (JES) and jet energy resolution (JER) measurement uncertainties on the expected signal $m_{\text{avg}}^{\text{jet}}$ distribution and the estimated background. The size of each mass window is defined to be equal to or larger than the full width of the $m_{\text{avg}}^{\text{jet}}$ mass spectrum for the $m_{\tilde{t}}$ model that best corresponds to that range. The definitions of

---

[3] This scattering angle, θ^*, is formed by boosting the two stop large-R jets to the centre-of-mass frame and measuring the angle of either stop large-R jet with respect to the beam line.
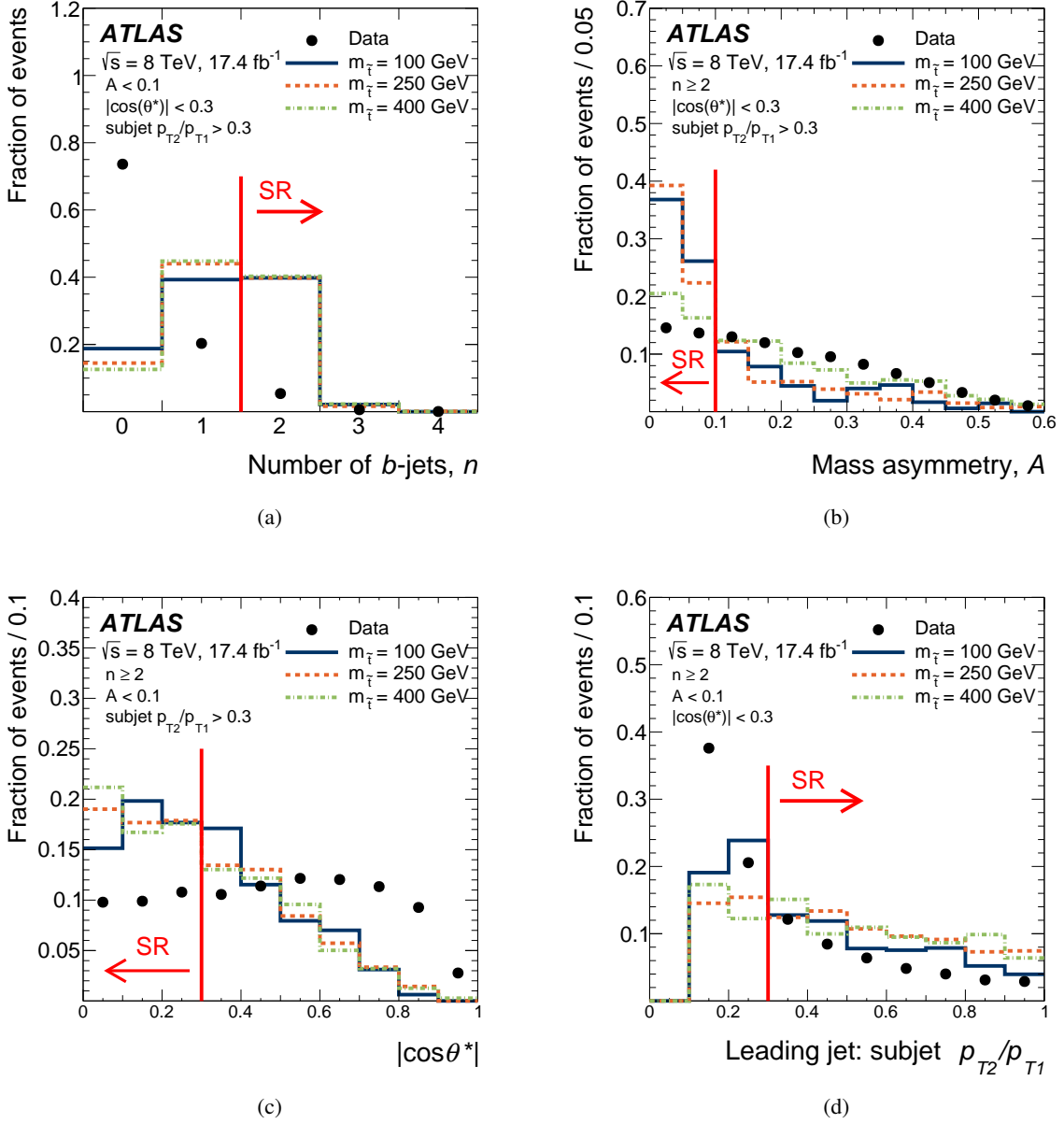
Figure 3: Distributions of the discriminating variables for events in which the other three selections are applied for each subfigure. The signal region is indicated with a red arrow. All distributions are normalised to unity. Overflows are included in the last bin for subfigures (a) and (b). (a) Number of b-tags/event, n. (b) Large-R jet mass asymmetry, $\mathcal{A}$. (c) Stop-pair centre-of-mass frame production angle, $|\cos\theta^*|$. (d) Subjet p_{T2}/p_{T1} for the leading jet in each event.

these mass windows and the signal efficiency in each window are given in Table 1. Figure 4(a) shows the mass windows overlaid on top of the signal $m_{\text{avg}}^{\text{jet}}$ distributions for a few stop masses. The efficiency of the mass windows (relative to the SR cuts of Eq. (5)) varies from 79% at 100 GeV to 19% at 400 GeV. The low efficiency at high mass is due to the fact that the decay products are often not fully contained in the large-R jet, as can be seen in Figure 4(b). Figure 5 shows the product of acceptance and efficiency, after

the SR cuts and mass windows, as a function of $m_{\tilde{t}}$. The significantly lower acceptance times efficiency for light stop masses in Figure 5 is almost entirely due to the efficiency of the trigger selections which are for 100, 250, and 400 GeV stop masses 0.56%, 22%, and 96%, respectively. This low efficiency is compensated by the large cross section for low stop masses retaining sensitivity to these mass values.
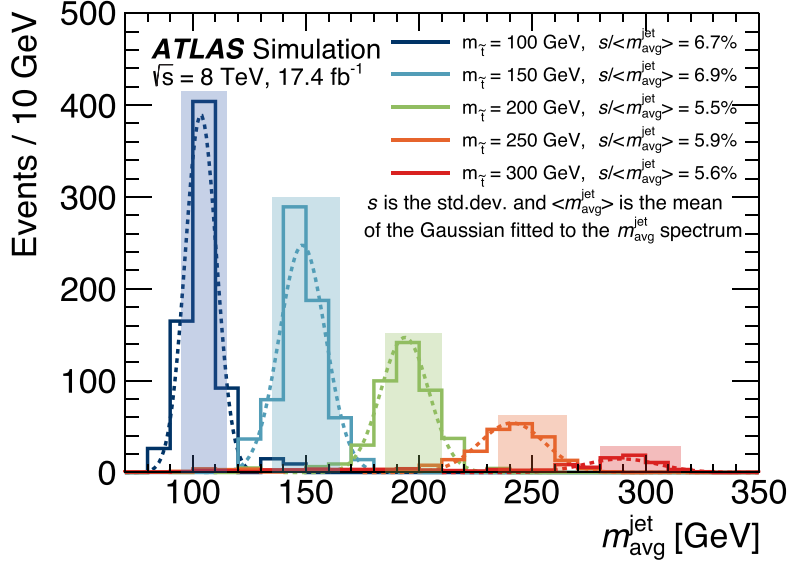
(a) Linear scale
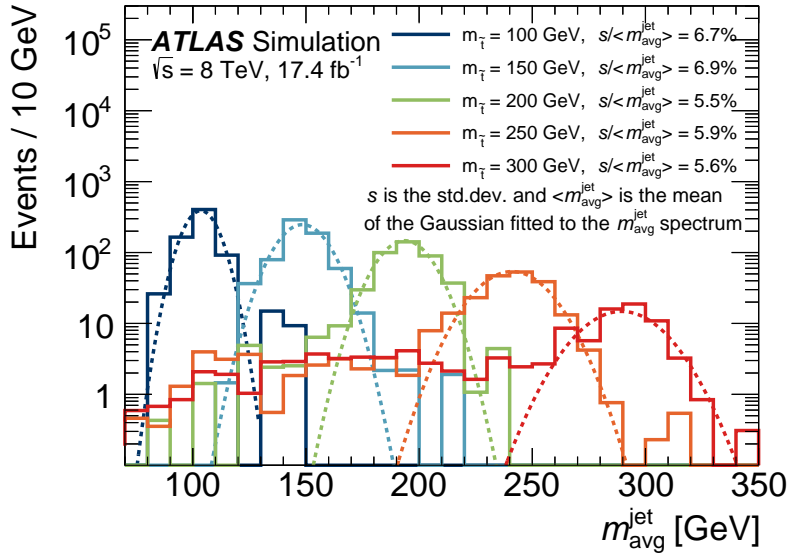
(b) Logarithmic scale

Figure 4: Distributions of the average jet mass $m_{\text{avg}}^{\text{jet}}$ for signal samples with $m_{\tilde{t}} = 100, 150, 200, 250,$ and 300 GeV, in linear (a) and logarithmic (b) scales (solid lines). A Gaussian distribution is fitted to the mass peak of each sample (dashed lines). The resolution, $s/\langle m_{\text{avg}}^{\text{jet}}\rangle$, is quoted for each stop mass value. The mass windows are highlighted with the shaded rectangles in (a). The long tail peaking around $m_{\tilde{t}}/2$ for high-mass stops shown in (b) is due to events where not all stop decay products are clustered within the large-R jets.

10

$m_{\tilde{t}}$ [GeV]	Window [GeV]	Selection efficiency in mass window
100	[95, 115]	79 %
125	[115, 135]	77 %
150	[135, 165]	83 %
175	[165, 190]	72 %
200	[185, 210]	68 %
225	[210, 235]	56 %
250	[235, 265]	55 %
275	[260, 295]	49 %
300	[280, 315]	44 %
325	[305, 350]	30 %
350	[325, 370]	29 %
375	[345, 395]	25 %
400	[375, 420]	19 %

Table 1: Definition of the signal mass windows and selection efficiency in each window relative to the SR cuts of Eq. (5).
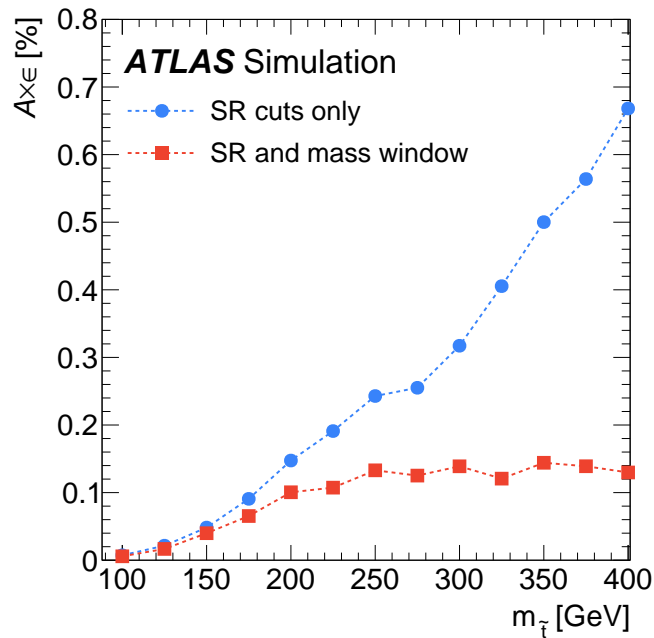
Figure 5: Total acceptance times efficiency ($A \times \epsilon$) of the SR cuts of Eq. (5), and SR cuts combined with the mass window selection in Table 1, as a function of $m_{\tilde{t}}$. The denominator of the efficiency (in %) is the total number of events, i.e. the top row in Table 3.

6 Background estimation

The estimation of the dominant SM multijet background in the signal region, including both the expected number of events and the shape of the $m_{\mathrm{avg}}^{\mathrm{jet}}$ background spectrum, is performed directly from the data. MC simulations are used to study the background estimation method itself and to assess the contribution from $t\bar{t}$ production. For the background estimation, additional kinematic regions are defined by inverting the $\mathcal{A}$ and $|\cos\theta^*|$ selections as shown in Table 2. These are labelled An, Bn, Cn, where n indicates the number of b-tags ($n = 0, = 1, \geq 2$). The signal region kinematic selection criteria of Eq. (5) are comprised by the Dn requirements and summarised in the last row of Table 2, where $SR \equiv D2$ with $n \geq 2$ b-tags, and $D1$ with $n = 1$ b-tag is a validation region. Signal event yields are summarised in Table 3 for three stop masses.

Region	$\mathcal{A}$	$|\cos\theta^*|$	Subjet $p_{\mathrm{T2}}/p_{\mathrm{T1}}$	n
An	≥ 0.1	≥ 0.3	> 0.3	$= 0, = 1, \geq 2$
Bn	< 0.1	≥ 0.3	> 0.3	$= 0, = 1, \geq 2$
Cn	≥ 0.1	< 0.3	> 0.3	$= 0, = 1, \geq 2$
Dn	< 0.1	< 0.3	> 0.3	$= 0, = 1, \geq 2$

Table 2: Definitions of the kinematic regions defined by $\mathcal{A}$, $|\cos\theta^*|$, subjet $p_{\mathrm{T2}}/p_{\mathrm{T1}}$, and the b-tag multiplicity ($n = 0, = 1, \geq 2$). The letters A, B, C, and D label the $\mathcal{A}$ and $|\cos\theta^*|$ selections, whereas n indicates the number of b-tags. $D2 \equiv SR$ is the signal region of the analysis.

The method relies on the assumption that the shape of the $m_{\mathrm{avg}}^{\mathrm{jet}}$ spectrum is independent of the various b-tagging selections, as Figure 6(a) indicates, in each of the kinematic regions (An, Bn, Cn, and Dn) defined in Table 2. The advantage of the approach adopted here is that events with fewer than two b-tagged jets can be used as control and validation regions for *in situ* studies of these kinematic regions. An estimation of the normalisation and shape of the spectrum in the signal region $D2$ can therefore be tested and validated using events with $n = 1$ as well as regions A ($\mathcal{A} \geq 0.1$, $|\cos\theta^*| \geq 0.3$) and C ($\mathcal{A} \geq 0.1$, $|\cos\theta^*| < 0.3$). Region B ($\mathcal{A} < 0.1$, $|\cos\theta^*| \geq 0.3$) is primarily used to evaluate shape differences in the predicted $m_{\mathrm{avg}}^{\mathrm{jet}}$ spectra (see Section 7.2).

The $\mathcal{A}$ and $|\cos\theta^*|$ variables are found to have a correlation coefficient of at most 1% in data events for $n = 0$. In simulated multijet events, the correlation is also consistent with zero in events with $n \geq 2$, within the large statistical uncertainties. Consequently, the ratio of $n \geq 2$ (or $n = 1$) to $n = 0$ in regions A, B, and C should be approximately the same as the ratio in region D. The average jet mass spectrum, $m_{\mathrm{avg}}^{\mathrm{jet}}$, is compared across the various n selections for region A, as well as between each of the regions in events with $n = 0$. These comparisons are shown in Figure 6 along with the ratio of the spectrum in each region to that which most closely matches the final signal region in each figure (region D for $n = 0$ and $n \geq 2$ for region A). The results demonstrate that the $m_{\mathrm{avg}}^{\mathrm{jet}}$ spectra in regions C and D are reliably reproduced by regions A and B, respectively, as shown in Figure 6(b).

The potential for events from $t\bar{t}$ production to contribute increases with the addition of b-tag-multiplicity selections. Table 4 presents the number of events in the data and the contribution from $t\bar{t}$, as determined

Selection	$m_{\tilde{t}} = 100$ GeV	$m_{\tilde{t}} = 250$ GeV	$m_{\tilde{t}} = 400$ GeV
Total events	$(9.72 \pm 0.01) \times 10^6$	$(9.54 \pm 0.02) \times 10^4$	$(6.202 \pm 0.002) \times 10^3$
Jet + H_T trigger	$(5.47 \pm 0.08) \times 10^4$	$(2.07 \pm 0.01) \times 10^4$	$(5.98 \pm 0.02) \times 10^3$
Large-R jet tag	$(1.68 \pm 0.04) \times 10^4$	$(4.76 \pm 0.06) \times 10^3$	$(1.29 \pm 0.01) \times 10^3$
$n \geq 2$	$(6.35 \pm 0.23) \times 10^3$	$(1.70 \pm 0.03) \times 10^3$	515 ± 6
A2	416 ± 58	194 ± 11	68.7 ± 2.2
B2	639 ± 71	199 ± 11	33.3 ± 1.6
C2	419 ± 62	149 ± 9	71.2 ± 2.2
D2	711 ± 74	240 ± 12	41.5 ± 1.8

Table 3: The expected number of signal events in 17.4 fb^{-1} from MC simulation for each of the selections applied to the $n \geq 2$ region. Stop masses of $m_{\tilde{t}} = 100$ GeV, 250 GeV and 400 GeV are shown. The statistical uncertainty of the MC simulation is shown for each selection. The jet + H_T trigger selection includes the offline selection. The large-R jet tag includes both the kinematic preselections and the *splitting* criteria defined by Eq. (1) and Eq. (2). No selections are placed on the masses of the candidate stop jets. The region definitions of A2–D2 are summarised in Table 2.

by MC simulation, in regions A, B, C, and D for $n = 0$, $= 1$, ≥ 2. The expected signal and $t\bar{t}$ contributions are also given for a few mass windows. The $t\bar{t}$ contribution is at the few per mille level in the events with $n = 0$. Contributions rise slightly in events with $n = 1$ to a maximum of $\lesssim 4\%$ in region $D1$. Lastly, regions $A2$ and $C2$ ($\mathcal{A} \geq 0.1$) have a maximum $t\bar{t}$ contribution of around $\lesssim 10\%$. Consequently, when validating the method and in the final background estimate, the contribution from $t\bar{t}$ is subtracted in each of the regions. The corrected total number of events in a given region is defined as $N_{Xn} = N_{Xn}^{\text{data}} - N_{Xn}^{t\bar{t}}$ and the corrected $m_{\text{avg}}^{\text{jet}}$ spectrum is defined as $N_{Xn,i} = N_{Xn,i}^{\text{data}} - N_{Xn,i}^{t\bar{t}}$, where i represents the ith bin of the histogram ($X = A, B, C,$ or D, and n refers to the number of b-tags). The two quantities are related by $N_{Xn} = \Sigma_i N_{Xn,i}$.

All regions used for the background estimation ($A0$, $C0$, $D0$, $A2$, and $C2$) exhibit potential signal contribution of less than 10%. Region $B2$ ($\mathcal{A} < 0.1$, $|\cos\theta^*| \geq 0.3$) is not used to derive the background estimate, since the expected signal contribution is much higher here than in $A2$ and $C2$ (for $m_{\tilde{t}} = 100$ GeV the signal contribution is 50% in $B2$, compared with 2.2% in $A2$ and 8.2% in $C2$). The expected signal contribution in the validation regions ($n = 1$) is only significant in $B1$ and $D1$ (both require $\mathcal{A} < 0.1$). Due to this level of expected signal contribution, and the $m_{\text{avg}}^{\text{jet}}$ dependence of that contribution, the background estimation procedure obtains the $m_{\text{avg}}^{\text{jet}}$ spectrum from the $n = 0$ regions for the final background spectrum estimate. The background estimation procedure itself is summarised in the following steps:

1. The $m_{\text{avg}}^{\text{jet}}$ shape ($N_{D0,i}$) and total number of events (N_{D0}) are extracted from the $D0$ region.

2. A projection factor is derived between events with $n = 0$ and events with $n \geq 2$ for the signal-depleted regions A ($\mathcal{A} \geq 0.1$, $|\cos\theta^*| \geq 0.3$) and C ($\mathcal{A} \geq 0.1$, $|\cos\theta^*| < 0.3$). As explained above,

13
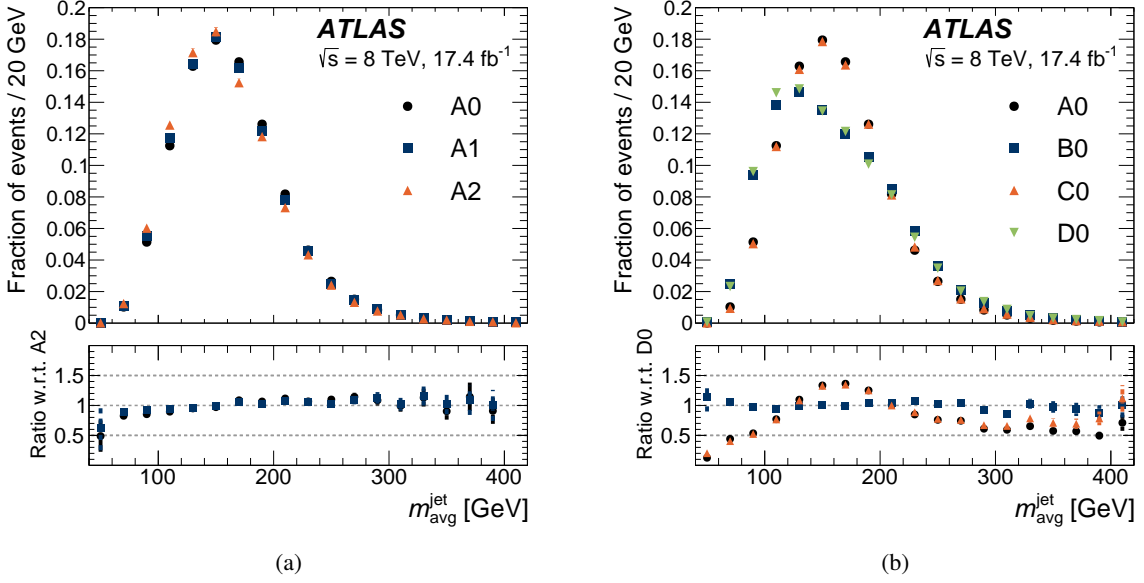
Figure 6: Shape comparisons of the $m_{\text{avg}}^{\text{jet}}$ spectrum for the data (a) in region A for events with $n = 0, = 1, \geq 2$ and (b) in regions A, B, C, D for events with $n = 0$. In each case, the lower panel shows the ratio of the spectrum in each region to that which most closely matches the final signal region ($n \geq 2$ for region A and region D for $n = 0$). Only statistical uncertainties are shown.

the number of $t\bar{t}$ events is subtracted in regions $A0, C0, A2,$ and $C2$ before evaluating the projection factor $\langle k_{A,C} \rangle_2$:

$$\langle k_{A,C} \rangle_2 = (k_{A2} + k_{C2})/2, \quad \text{where} \quad k_{X2} = \frac{N_{X2}}{N_{X0}}, \quad X = A, C. \tag{6}$$

3. The projection factor is used to estimate the total number of events,

$$N'_{D2} = \langle k_{A,C} \rangle_2 \times N_{D0} + N_{D2}^{t\bar{t}}, \tag{7}$$

and shape (bin-by-bin),

$$N'_{D2,i} = \langle k_{A,C} \rangle_2 \times N_{D0,i} + N_{D2,i}^{t\bar{t}}, \tag{8}$$

in the signal region, $D2$ (where the contribution from $t\bar{t}$ in $D2$ has been added).

This procedure is performed in the entire mass range and the mass windows are then defined from the estimated background spectrum. The projection factors k_{A2} and k_{C2} are compatible at the level of about 4% (including the $t\bar{t}$ subtraction as in Eq. (6)) and this difference is included as a systematic uncertainty on the background estimate (see Section 7). The validity of the background estimation method can be demonstrated in the $n = 1$ regions by deriving a projection factor analogously to Eq. (6) for $n = 0$ and $n = 1$,

$$\langle k_{A,C} \rangle_1 = (k_{A1} + k_{C1})/2. \tag{9}$$

The expected number of events in the full range of $D1$ is then estimated by

$$\begin{aligned} N'_{D1} &= \langle k_{A,C} \rangle_1 \times N_{D0} + N_{D1}^{t\bar{t}} \\ &= 12400 \pm 130. \end{aligned} \tag{10}$$

14

Region	N_{data}	$N_{t\bar{t}}$ ($\pm$ stat. $\pm$ syst.)		[95, 115] GeV		[135, 165] GeV		[165, 190] GeV		[375, 420] GeV	
				$\frac{N_S}{N_{\text{data}}}$	$\frac{N_{t\bar{t}}}{N_{\text{data}}}$	$\frac{N_S}{N_{\text{data}}}$	$\frac{N_{t\bar{t}}}{N_{\text{data}}}$	$\frac{N_S}{N_{\text{data}}}$	$\frac{N_{t\bar{t}}}{N_{\text{data}}}$	$\frac{N_S}{N_{\text{data}}}$	$\frac{N_{t\bar{t}}}{N_{\text{data}}}$
						$n = 0$					
N_{A0}	296 226	390 $\pm$ 10	$^{+100}_{-95}$	0.21 %	0.27 %	0.048 %	0.14 %	0.019 %	0.072 %	0.11 %	0.037 %
N_{B0}	115 671	176 $\pm$ 7	$^{+50}_{-42}$	0.64 %	0.20 %	0.90 %	0.17 %	0.50 %	0.14 %	0.68 %	0.13 %
N_{C0}	114 186	221 $\pm$ 8	$^{+59}_{-52}$	0.42 %	0.39 %	0.088 %	0.20 %	0.020 %	0.093 %	0.24 %	0.18 %
N_{D0}	44 749	110 $\pm$ 6	$^{+27}_{-27}$	4.0 %	0.27 %	2.0 %	0.29 %	2.3 %	0.24 %	2.4 %	0. %
						$n = 1$					
N_{A1}	79 604	1 110 $\pm$ 10	$^{+190}_{-180}$	1.2 %	2.6 %	0.46 %	1.5 %	0.48 %	0.74 %	0.22 %	0.71 %
N_{B1}	31 045	517 $\pm$ 11	$^{+84}_{-83}$	14 %	1.9 %	9.7 %	2.3 %	8.0 %	1.9 %	10 %	0.089 %
N_{C1}	32 163	620 $\pm$ 10	$^{+110}_{-100}$	4.8 %	3.4 %	1.6 %	2.1 %	1.3 %	0.99 %	0.28 %	0.76 %
N_{D1}	12 350	306 $\pm$ 8	$^{+52}_{-45}$	29 %	2.3 %	31 %	3.6 %	21 %	3.7 %	43 %	0.000 10 %
						$n \geq 2$					
N_{A2}	22 259	1 050 $\pm$ 10	$^{+190}_{-170}$	2.2 %	6.8 %	1.7 %	5.7 %	1.2 %	2.8 %	1.0 %	1.9 %
N_{B2}	8 416	556 $\pm$ 10	$^{+94}_{-86}$	50 %	7.2 %	29 %	10 %	24 %	8.8 %	26 %	0.24 %
N_{C2}	9 384	570 $\pm$ 10	$^{+100}_{-94}$	8.2 %	8.8 %	4.1 %	7.5 %	2.8 %	2.9 %	2.8 %	2.7 %
N_{D2}	3 688	311 $\pm$ 7	$^{+60}_{-47}$	120 %	8.4 %	73 %	14 %	72 %	11 %	160 %	0.51 %

Table 4: The observed event yields for 17.4 fb^{-1} in each of the regions for each b-tag multiplicity are shown, as well as the expected fractional signal contribution for the mass windows (as defined in Table 1) corresponding to $m_{\tilde{t}} = 100$, 150, 175, and 400 GeV, and the $t\bar{t}$ contribution in the same mass windows. The $t\bar{t}$ systematic uncertainties include both the detector-level uncertainties and the theoretical uncertainties, as described in Section 7.

The same estimate for $D2$ gives

$$
\begin{aligned}
N'_{D2} &= \langle k_{A,C}\rangle_2 \times N_{D0} + N^{t\bar{t}}_{D2} \\
&= 3640^{+90}_{-80}.
\end{aligned}
\tag{11}
$$

In Eq. (10) and Eq. (11) the uncertainty quoted includes the statistical uncertainty and the uncertainties related to the $t\bar{t}$ estimate (see Section 7). These numbers should be compared with the observed numbers of events in Table 4, 12350 in $D1$ and 3688 in $D2$. The observed numbers of events are consistent with the estimated values.

7 Systematic uncertainties

Several sources of systematic uncertainty are considered when determining the estimated contributions from signal and background. The background estimate uncertainties pertain primarily to the method itself. The control and validation regions defined in Section 6 are used to evaluate the size of these uncertainties. A description of the primary sources of uncertainty follows.

7.1 *b*-jet-multiplicity $m_{\mathrm{avg}}^{\mathrm{jet}}$ shape uncertainty

Regions A ($\mathcal{A} \geq 0.1$, $|\cos\theta^*| \geq 0.3$) and C ($\mathcal{A} \geq 0.1$, $|\cos\theta^*| < 0.3$) are used to directly compare the shape of the $m_{\mathrm{avg}}^{\mathrm{jet}}$ spectrum in events with *b*-jet-multiplicities of $n = 0$ and $n \geq 2$ (the $t\bar{t}$-corrected $m_{\mathrm{avg}}^{\mathrm{jet}}$ spectrum is used, as defined in Section 6). The *b*-jet-multiplicity $m_{\mathrm{avg}}^{\mathrm{jet}}$ shape systematic uncertainty is calculated as the maximum of the bin-by-bin difference of region $A2$ compared to $A0$ (Figure 6(a)) and $C2$ compared to $C0$,

$$\sigma_i^{b-\mathrm{jet-multi.\ syst.}} = \max\left[|1 - v_{A2,i}/v_{A0,i}|, |1 - v_{C2,i}/v_{C0,i}|\right], \tag{12}$$

where the normalised $m_{\mathrm{avg}}^{\mathrm{jet}}$ spectrum are defined as $v_{Xn,i} = N_{Xn,i}/N_{Xn}$ ($X = A, C$). The expression in Eq. (12) is then added in quadrature with the statistical uncertainty to form the total systematic uncertainty for that particular bin. A fixed bin width of 50 GeV is used in order to reduce effects due to statistical uncertainties. The size of the *b*-jet-multiplicity $m_{\mathrm{avg}}^{\mathrm{jet}}$ shape systematic uncertainty varies from approximately 7–12% at low $m_{\mathrm{avg}}^{\mathrm{jet}}$ to 20% near $m_{\mathrm{avg}}^{\mathrm{jet}} \approx 300$ GeV, and to around 90% for $m_{\mathrm{avg}}^{\mathrm{jet}} \approx 400$ GeV. The large systematic uncertainty in the high-mass tail is due to the low number of events in the $n \geq 2$ regions. Figure 8 shows the *b*-jet-multiplicity $m_{\mathrm{avg}}^{\mathrm{jet}}$ shape systematic uncertainty as well as the total systematic uncertainty when combined with the constant systematic uncertainty due to the 4% difference between projection factors k_{A2} and k_{C2} mentioned in Section 6, and the background estimation $m_{\mathrm{avg}}^{\mathrm{jet}}$ shape systematic uncertainty described below in Section 7.2.

7.2 Background estimation $m_{\mathrm{avg}}^{\mathrm{jet}}$ shape uncertainty

Events with $n = 1$ are used to test the validity of the background estimation method in data and to derive a systematic uncertainty on the approach. Figure 7 shows several results of this test by comparing three estimated spectra with the observed spectrum in each of the four regions. The estimated spectra of Figure 7 are determined using projection factors,

$$k_{X1} = N_{X1}/N_{X0}, \tag{13}$$

from events with $n = 0$ to those with $n = 1$, in each of the three regions $X = A$, B, and C in order to determine the extent to which the prediction varies with each choice. Region $D1$ was used to validate the systematic uncertainty derived from $A1$, $B1$, and $C1$. Because of the three projection factors (k_A, k_B, and k_C) there are three estimates ($N_{Y1'_A,i}$, $N_{Y1'_B,i}$, and $N_{Y1'_C,i}$) of the $m_{\mathrm{avg}}^{\mathrm{jet}}$ spectrum in each of the regions $Y1 = A1$, $B1$, and $C1$. Thus, in total there are nine estimates of the actual spectra, these are written succinctly as

$$N_{Y1'_X,i} = k_{X1} \times N_{Y0,i}, \text{ where } X = \{A, B, C\} \text{ and } Y = \{A, B, C\}. \tag{14}$$

These estimates provide a test of the shape compatibility as well as the overall normalisation of the background estimate (the special cases $N_{A1'_A,i}$, $N_{B1'_B,i}$, and $N_{C1'_C,i}$ are normalised to the data by construction and thus only provide a shape comparison of $n = 1$ and $n = 0$). A systematic uncertainty for the background projection is then derived by taking, bin-by-bin, the largest deviation of the ratio of estimated to actual yield from unity in the $m_{\mathrm{avg}}^{\mathrm{jet}}$ spectra in each of the regions A, B, and C according to

$$\sigma_i^{\mathrm{bkg.\ syst.}} = \max_{X,Y}\left[|1 - N_{Y1'_X,i}/N_{Y1,i}|\right], \tag{15}$$

where $N_{Y1,i}$ are the observed data points and $N_{Y1'_X,i}$ are the estimated spectra defined by Eq. (14). A bin width of 50 GeV is used, just as above with the b-jet multiplicity $m_{\mathrm{avg}}^{\mathrm{jet}}$ shape systematic uncertainty. This is added in quadrature with the statistical uncertainty of that ratio in order to form the total systematic uncertainty for that particular bin. The size of the background estimation $m_{\mathrm{avg}}^{\mathrm{jet}}$ shape systematic uncertainty varies from less than 10% at low $m_{\mathrm{avg}}^{\mathrm{jet}} \approx 100$ GeV to 20% near $m_{\mathrm{avg}}^{\mathrm{jet}} \approx 400$ GeV. Figure 8 shows the background estimation $m_{\mathrm{avg}}^{\mathrm{jet}}$ shape systematic uncertainty as well as the total systematic uncertainty when combined with the two above-mentioned systematic uncertainties.

(a) Region A

(b) Region B
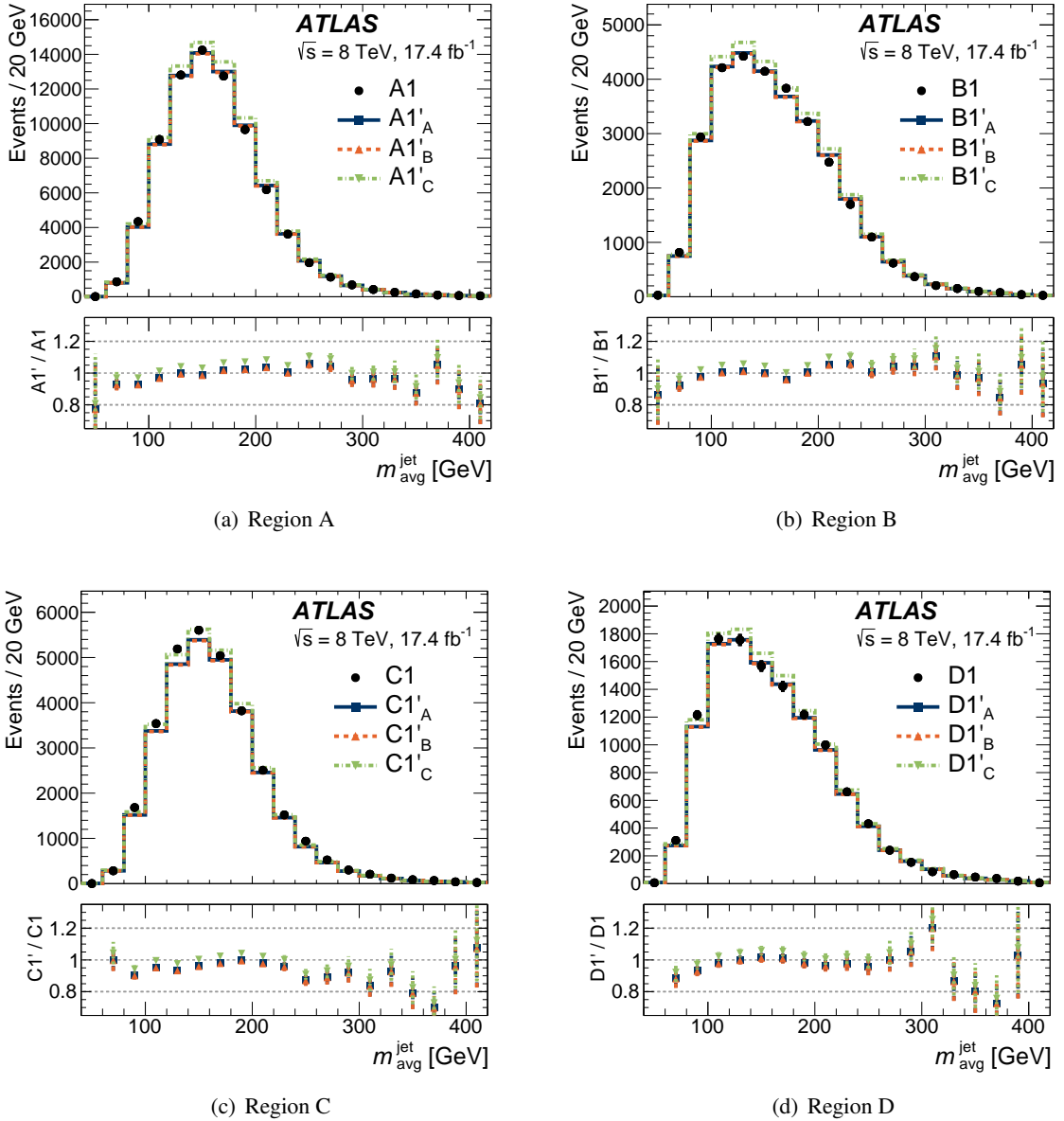
(c) Region C

(d) Region D

Figure 7: The $m_{\mathrm{avg}}^{\mathrm{jet}}$ distribution is shown in four validation regions with $n = 1$. In each case the data ($A1$, $B1$, $C1$, and $D1$) are compared to estimates based on projection factors derived between $n = 0$ and $n = 1$ in A, B, and C (see Section 7.2).

17
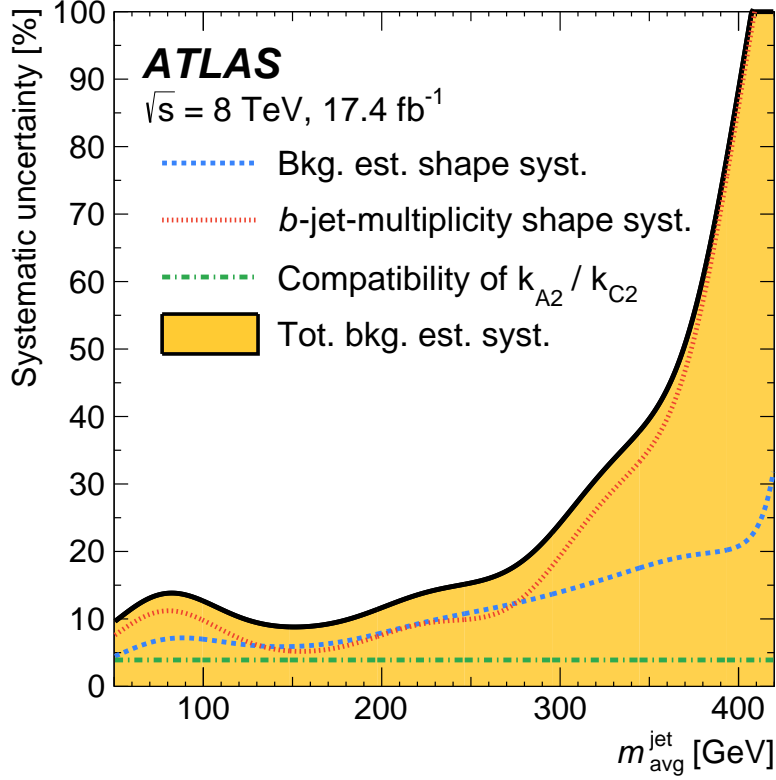
Figure 8: Systematic uncertainty for the data-driven multijet background estimation. The blue dashed line represents the background estimation systematic uncertainty estimated from comparisons of the predicted $m_{\mathrm{avg}}^{\mathrm{jet}}$ spectra in regions $A1$, $B1$, and $C1$ to the actual spectra. The red dotted line represents the estimated systematic uncertainty due to shape differences between events with $n = 0$ and $n \geq 2$. The green line represents a systematic uncertainty due to the level of compatibility of k_{A2} and k_{C2}. Finally, the black line with a filled yellow area shows the combined systematic uncertainty of all three contributions added in quadrature. The systematic uncertainty curves were smoothed with a Gaussian filter of spread 20 GeV.

7.3 Background $t\bar{t}$ contribution systematic uncertainty

Since POWHEG+PYTHIA MC simulation is used to determine the contribution from $t\bar{t}$ events in the signal region and each of the control regions, systematic uncertainties related to the MC simulation of the process itself are included in the total systematic uncertainty for the background estimation. The theoretical uncertainties include renormalisation and factorisation scale variations, parton distribution function uncertainties, the choice of MC generator using comparisons with MC@NLO [95], the choice of parton shower models using comparisons with Herwig [96], and initial- and final-state radiation (FSR) modelling uncertainties. The size of the theoretical systematic uncertainties for $t\bar{t}$ production vary from approximately 40% to 70% in the relevant kinematic regions and are dominated by the uncertainties from the MC generator and ISR/FSR variations. The detector-level uncertainties include the JES and JER uncertainties [83] as well as the b-tagging efficiency and mistag-rate uncertainties [87]. Uncertainties associated with the large-R jet mass scale and resolution are taken into account by the JES and JER uncertainties of the input small-R jets [88].

The size of the total $t\bar{t}$ systematic uncertainty varies in the mass range $m_{\mathrm{avg}}^{\mathrm{jet}}$ = 100–200 GeV from approximately 50% to 80%. In the range $m_{\mathrm{avg}}^{\mathrm{jet}}$ = 300–400 GeV the $t\bar{t}$ systematic uncertainties are of the order of 100%, but the $t\bar{t}$ background is completely negligible in this range. Lastly, an uncertainty of 2.8% is applied to the measured integrated luminosity of 17.4 fb^{-1} following the methodology described in Ref. [97].

7.4 Signal systematic uncertainties

In addition to the systematic uncertainties associated with the background estimate, the MC simulation of the signal model is subject to systematic uncertainties. Much like the contribution from $t\bar{t}$, these uncertainties include experimental uncertainties as well as theoretical uncertainties. The detector-level uncertainties include the JES and JER uncertainties, and the b-tagging uncertainties as described for the estimate of $t\bar{t}$. The theoretical uncertainties include renormalisation and factorisation scale variations, parton distribution function uncertainties, and ISR and FSR modelling uncertainties. The nominal signal cross-section and its uncertainty are taken from an envelope of cross-section predictions using different PDF sets and factorisation and renormalisation scales, as described in Ref. [66]. Each signal model is varied according to these systematic uncertainties and the impact on the acceptance in each mass window is then propagated to the final result. The largest contribution to the total signal systematic uncertainty comes from the JES and b-tagging, both in the range 10–18%. The size of the theoretical uncertainty grows from around 5% for low-mass stops to around 10% for higher-mass stops.

To evaluate the ISR/FSR systematic uncertainty, separate samples of $\widetilde{t}\widetilde{t}^{*}$ pair events are generated using MadGraph +PYTHIA, and the rate of ISR/FSR production is varied. These are used to reweight the $p_{\mathrm{T}}(\widetilde{t}\widetilde{t}^{*})$ distribution of the nominal signal samples to estimate the change in signal acceptance × efficiency. The effect ranges from 0–17%, with the largest impact at high $m_{\widetilde{t}}$.

8 Results

Table 5 summarises the observed and expected number of events that fall within each of the optimised mass windows in the signal region, $D2$. Figure 9 shows the observed $m_{\mathrm{avg}}^{\mathrm{jet}}$ distribution in the data, along with the estimated background spectrum, including both the systematic and statistical uncertainties. No excess over the background prediction is observed.

Model-independent upper limits at 95% confidence level (CL) on the number of beyond-the-SM (BSM) events for each signal region are derived using the CL$_s$ prescription [98] and neglecting any possible contribution in the control regions. Dividing these by the integrated luminosity of the data sample provides upper limits on the visible BSM cross-section, $\sigma_{\mathrm{vis.}}$, which is defined as the product of acceptance (A), reconstruction efficiency (ϵ), branching ratio (BR), and production cross-section ($\sigma_{\mathrm{prod.}}$). This search specifically targets low-mass $\widetilde{t} \to \bar{b}\bar{s}$ decays, assuming 100% BR. The resulting limits on the number of BSM events and on the visible signal cross-section are shown in Table 6. The significance of an excess can be quantified by the probability (p_0) that a background-only experiment has at least as many events as observed. This p-value is also reported for each region in Table 6, where $p_0 = 1 - \mathrm{CL}_b$ and CL_b is the confidence level observed for the background-only hypothesis. The p-value is truncated at 0.5 for any signal region where the observed number of events is less than the expected number.

$m_{\tilde{t}}$ [GeV]	Window [GeV]	$N_B^{\text{data-driven est.}}$	$N_B^{t\bar{t}\,\text{est.}}$	$N_B^{\text{tot. est.}}$	$N_{\text{data}}^{\text{obs.}}$	N_S
100	[95, 115]	465 ± 56	39 ± 26	504 ± 61	460	560 ± 140
125	[115, 135]	496 ± 49	68 ± 37	564 ± 61	555	570 ± 130
150	[135, 165]	680 ± 61	105 ± 49	785 ± 78	761	560 ± 110
175	[165, 190]	471 ± 46	63 ± 19	534 ± 50	583	421 ± 96
200	[185, 210]	395 ± 46	16.5 ± 9.6	412 ± 47	416	293 ± 50
225	[210, 235]	266 ± 37	2.4 ± 2.4	269 ± 37	283	178 ± 36
250	[235, 265]	176 ± 27	1.1 ± 1.1	177 ± 27	195	127 ± 29
275	[260, 295]	104 ± 19	0.59 ± 0.55	104 ± 19	96	71 ± 20
300	[280, 315]	69 ± 16	0.93 ± 0.29	70 ± 16	51	48 ± 10
325	[305, 350]	43 ± 14	0.73 ± 0.53	43 ± 14	44	29.4 ± 6.9
350	[325, 370]	26 ± 10	0.23 ± 0.15	26 ± 10	37	20.2 ± 4.3
375	[345, 395]	18.6 ± 9.8	0.076 ± 0.076	18.7 ± 9.8	22	12.6 ± 2.8
400	[375, 420]	9.5 ± 7.7	0.026 ± 0.026	9.5 ± 7.7	5	8.1 ± 1.8

Table 5: Summary of the observed number of events in the data and the estimated number of signal and background events with total uncertainties (i.e. all listed uncertainties are the combined statistical and systematic uncertainties) that fall within each of the optimised mass windows in region $D2$. The total number of estimated background events in each window is the sum of the estimated background from the data-driven method and the $t\bar{t}$ simulation. The columns, from left to right indicate: $N_B^{\text{data-driven est.}}$, the data-driven background estimate; $N_B^{t\bar{t}\,\text{est.}}$, the background contribution from $t\bar{t}$; $N_B^{\text{tot. est.}}$, the total estimated background; $N_{\text{data}}^{\text{obs.}}$, the number of observed events in the data; and N_S, the number of expected signal events.

Exclusion limits are set on the signal model of interest. A profile likelihood ratio combining Poisson probabilities for signal and background is computed to determine the 95% CL for compatibility of the data with the signal-plus-background hypothesis (CL_{s+b}) [99]. A similar calculation is performed for the background-only hypothesis (CL_b). From the ratio of these two quantities, the confidence level for the presence of signal (CL_s) is determined [98]. Systematic uncertainties are treated as nuisance parameters assuming Gaussian distributions and pseudo-experiments are used to evaluate the results. This procedure is implemented using a software framework for statistical data analysis, HistFitter [100]. The observed and expected 95% CL upper limits on the allowed cross-section are shown in Figure 10. For each simulated stop mass, the optimal mass window is chosen and the expected background yield is compared to the observed number of events in the mass window. Any potential signal contribution in the control regions from which the background estimates are derived is included as a systematic uncertainty on the background estimate. The size of the potential signal contribution in the control regions is shown for a few mass windows in Table 4. Stops with masses between $100 \le m_{\tilde{t}} \le 315$ GeV are excluded at 95% confidence level. All mass limits are quoted using the $\tilde{t}\tilde{t}^*$ signal production cross-section reduced by one standard deviation of the theory uncertainties.

	Model-independent upper limits at 95% CL			
Window [GeV]	$\sigma_{\text{vis.}}$ [fb]	Observed N_{BSM}	Expected N_{BSM}	p_0
[95, 115]	5.8	101	$127 \; ^{+50}_{-36}$	0.50
[115, 135]	7.0	122	$128 \; ^{+50}_{-36}$	0.50
[135, 165]	8.4	145	$160 \; ^{+40}_{-45}$	0.50
[165, 190]	8.4	146	$109 \; ^{+43}_{-31}$	0.19
[185, 210]	5.9	103	$100 \; ^{+39}_{-28}$	0.47
[210, 235]	5.1	89	$79 \; ^{+31}_{-22}$	0.36
[235, 265]	4.2	73	$60 \; ^{+24}_{-17}$	0.28
[260, 295]	2.2	38	$43 \; ^{+17}_{-12}$	0.50
[280, 315]	1.4	25	$35 \; ^{+14}_{-10}$	0.50
[305, 350]	1.7	30	$30 \; ^{+12}_{-8}$	0.49
[325, 370]	1.8	31.8	$23.5 \, ^{+9.4}_{-6.6}$	0.18
[345, 395]	1.4	23.8	$21.4 \, ^{+8.4}_{-6.0}$	0.38
[375, 420]	0.57	10.0	$10.8 \, ^{+3.2}_{-2.1}$	0.50

Table 6: Left to right: mass window range, 95% CL upper limits on the visible cross-section ($\sigma_{\text{vis.}} = \langle A \times \epsilon \times \text{BR} \times \sigma_{\text{prod.}} \rangle$) and on the number of signal events (Observed N_{BSM}). The fourth column (Expected N_{BSM}) shows the 95% CL upper limit on the number of signal events, given the expected number (and $\pm 1\sigma$ excursions on the expectation) of background events. The last column indicates the discovery p-value, $p_0 = 1 - \text{CL}_b$, where CL_b is the confidence level observed for the background-only hypothesis. The p-value is truncated at 0.5 for any mass window where the observed number of events is less than the expected number.
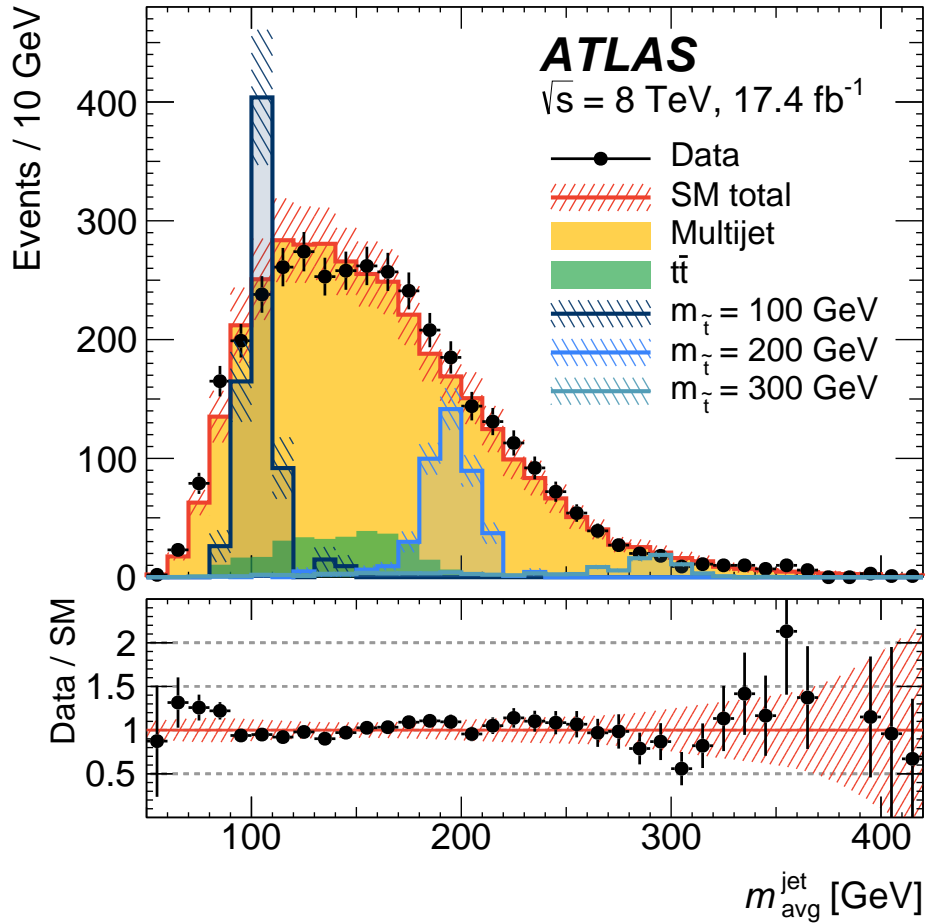
Figure 9: The observed m_{avg}^{jet} spectrum in the signal region is shown as black points with statistical uncertainties. Also shown is the total SM background estimate, and the separate contributions from the data-driven multijet and MC $t\bar{t}$ backgrounds. The red hatched band represents the combined statistical and systematic uncertainty on the total SM background estimate. Signal mass spectra are shown with statistical uncertainties only. The bottom panel shows the ratio of the data relative to the total SM background estimate.
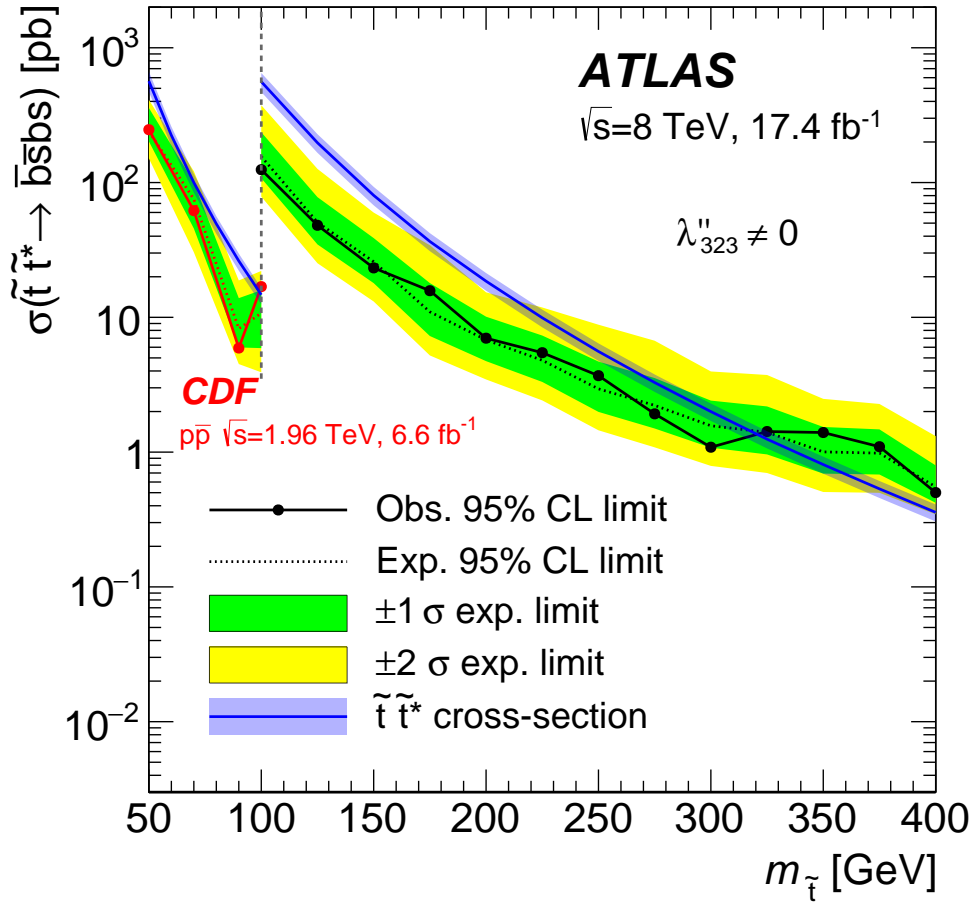
Figure 10: Observed and expected 95% CL upper limits on the stop pair production cross-section as function of the stop mass. The solid line with big round markers shows the observed limit, the dotted line shows the expected exclusion limit, and the green and yellow bands represent the uncertainties on this limit. Limits from the CDF Collaboration are shown in red for $m_{\tilde{t}} \leq 100$ GeV [40]. The blue line shows the theoretical signal cross-section and the blue band indicates the $\pm 1\sigma$ variations due to theoretical uncertainties on the signal production cross-section given by renormalisation and factorisation scale and PDF uncertainties. For this search the cross-section is calculated at NLO+NLL, whereas in the CDF paper the cross-section was calculated at NLO only.

9 Conclusions

This paper presents a search for direct pair production of light top squarks, decaying via an *R*-parity-violating coupling to *b*- and *s*-quarks. This leads to a final state characterised by two large-radius hadronic jets that each contain both decay products of the top squark. The search uses 17.4 fb^{-1} of $\sqrt{s} = 8$ TeV proton–proton collision data collected with the ATLAS detector at the LHC. No deviation from the background prediction is observed, and top squarks with masses between 100 and 315 GeV are excluded at 95% confidence level.

10 Acknowledgements

References

[1] Y. A. Gol'fand and E. P. Likhtman, *Extension of the Algebra of Poincare Group Generators and Violation of p Invariance*, JETP Lett. **13** (1971) 323, [Pisma Zh. Eksp. Teor. Fiz. 13:452-455. 1971].

[2] D. V. Volkov and V. P. Akulov, *Is the Neutrino a Goldstone Particle?*, Phys. Lett. B **46** (1973) 109.

[3] J. Wess and B. Zumino, *Supergauge Transformations in Four-Dimensions*, Nucl. Phys. B **70** (1974) 39.

[4] J. Wess and B. Zumino, *Supergauge Invariant Extension of Quantum Electrodynamics*, Nucl. Phys. B **78** (1974) 1.

[5] S. Ferrara and B. Zumino, *Supergauge Invariant Yang-Mills Theories*, Nucl. Phys. B **79** (1974) 413.

[6] A. Salam and J. A. Strathdee, *Supersymmetry and Nonabelian Gauges*, Phys. Lett. B **51** (1974) 353.

[7] S. P. Martin, *A Supersymmetry primer*, arXiv:hep-ph/9709356 [hep-ph], [Adv. Ser. Direct. High Energy Phys.18,1(1998)].

[8] N. Sakai, *Naturalness in Supersymmetric GUTs*, Zeit. Phys. C **11** (1981) 153.

[9] S. Dimopoulos, S. Raby, and F. Wilczek, *Supersymmetry and the Scale of Unification*, Phys. Rev. D **24** (1981) 1681.

[10] L. E. Ibanez and G. G. Ross, *Low-Energy Predictions in Supersymmetric Grand Unified Theories*, Phys. Lett. B **105** (1981) 439.

[11] S. Dimopoulos and H. Georgi, *Softly Broken Supersymmetry and SU(5)*, Nucl. Phys. B **193** (1981) 150.

[12] H. Goldberg, *Constraint on the photino mass from cosmology*, Phys. Rev. Lett. **50** (1983) 1419.

[13] J. Ellis, J. Hagelin, D. Nanopoulos, K. Olive, and M. Srednicki, *Supersymmetric relics from the big bang*, Nucl. Phys. B **238** (1984) 453.

[14] G. R. Farrar and P. Fayet, *Phenomenology of the Production, Decay, and Detection of New Hadronic States Associated with Supersymmetry*, Phys. Lett. B **76** (1978) 575.

[15] ATLAS Collaboration, *ATLAS Run 1 searches for direct pair production of third-generation squarks at the Large Hadron Collider*, Eur. Phys. J. C **75** (2015) 510, arXiv:1506.08616 [hep-ex].

[16] CMS Collaboration, *Searches for third-generation squark production in fully hadronic final states in proton-proton collisions at $\sqrt{s}$ = 8 TeV*, JHEP **1506** (2015) 116, arXiv:1503.08037 [hep-ex].

[17] ATLAS Collaboration, *Search for a Heavy Neutral Particle Decaying to eμ, eτ, or μτ in pp Collisions at $\sqrt{s}$ = 8 TeV with the ATLAS Detector*, Phys. Rev. Lett. **115** (2015) 031801, arXiv:1503.04430 [hep-ex].

[18] ATLAS Collaboration, *Search for long-lived stopped R-hadrons decaying out-of-time with pp collisions using the ATLAS detector*, Phys. Rev. D **88** (2013) 112003, `arXiv:1310.6584 [hep-ex]`.

[19] ATLAS Collaboration, *Searches for heavy long-lived charged particles with the ATLAS detector in proton–proton collisions at $\sqrt{s}$ = 8 TeV*, JHEP **1501** (2015) 068, `arXiv:1411.6795 [hep-ex]`.

[20] ATLAS Collaboration, *Search for massive, long-lived particles using multitrack displaced vertices or displaced lepton pairs in pp collisions at $\sqrt{s}$ = 8 TeV with the ATLAS detector*, Phys. Rev. D **92** (2015) 072004, `arXiv:1504.05162 [hep-ex]`.

[21] ATLAS Collaboration, *Search for metastable heavy charged particles with large ionisation energy loss in pp collisions at $\sqrt{s}$ = 8 TeV using the ATLAS experiment*, Eur. Phys. J. C **75** (2015) 407, `arXiv:1506.05332 [hep-ex]`.

[22] ATLAS Collaboration, *Search for supersymmetry in events with four or more leptons in $\sqrt{s}$ = 8 TeV pp collisions with the ATLAS detector*, Phys. Rev. D **90** (2014) 052001, `arXiv:1405.5086 [hep-ex]`.

[23] CMS Collaboration, *Search for top squarks in R-parity-violating supersymmetry using three or more leptons and b-tagged jets*, Phys. Rev. Lett. **111** (2013) 221801, `arXiv:1306.6643 [hep-ex]`.

[24] ATLAS Collaboration, *Search for massive supersymmetric particles decaying to many jets using the ATLAS detector in pp collisions at $\sqrt{s}$ = 8 TeV*, Phys. Rev. D **91** (2015) 112016, `arXiv:1502.05686 [hep-ex]`.

[25] K. Inoue, A. Kakuto, H. Komatsu, and S. Takeshita, *Aspects of Grand Unified Models with Softly Broken Supersymmetry*, Prog. Theor. Phys. **68** (1982) 927, [Erratum: Prog. Theor. Phys.70,330(1983)].

[26] J. R. Ellis and S. Rudaz, *Search for Supersymmetry in Toponium Decays*, Phys. Lett. B **128** (1983) 248.

[27] R. Barbieri and G. Giudice, *Upper Bounds on Supersymmetric Particle Masses*, Nucl. Phys. B **306** (1988) 63.

[28] B. de Carlos and J. Casas, *One loop analysis of the electroweak breaking in supersymmetric models and the fine tuning problem*, Phys. Lett. B **309** (1993) 320, `arXiv:hep-ph/9303291 [hep-ph]`.

[29] H. K. Dreiner, *An introduction to explicit R-parity violation*, Pramana **51** (1998) 123–133, `arXiv:hep-ph/9707435 [hep-ph]`.

[30] B. Allanach, A. Dedes, and H. Dreiner, *R parity violating minimal supergravity model*, Phys. Rev. D **69** (2004) 115002, `arXiv:hep-ph/0309196 [hep-ph]`.

[31] B. Allanach, A. Dedes, and H. K. Dreiner, *Bounds on R-parity violating couplings at the weak scale and at the GUT scale*, Phys. Rev. D **60** (1999) 075014, `arXiv:hep-ph/9906209 [hep-ph]`.

[32] M. Sher and J. L. Goity, *Bounds on Delta B = 1 Couplings in the Supersymmetric Standard Model*, Phys. Lett. B **346** (1995) 69, `arXiv:hep-ph/9503472 [hep-ph]`.

[33] F. Zwirner, *Observable ΔB = 2 transitions without nucleon decay in a minimal supersymmetric extension of the Standard Model*, Phys. Lett. B **132** (1983) 103.

[34] G. Bhattacharyya, *A Brief review of R-parity violating couplings (Invited talk presented at 'Beyond the Desert', Castle Ringberg, Tegernsee, Germany, 8-14 June 1997)*, `arXiv:hep-ph/9709395 [hep-ph]`.

[35] G. D'Ambrosio, G. F. Giudice, G. Isidori, and A. Strumia, *Minimal flavor violation: An Effective field theory approach*, Nucl. Phys. B **645** (2002) 155–187, `arXiv:hep-ph/0207036 [hep-ph]`.

[36] B. Batell, T. Lin, and L.-T. Wang, *Flavored Dark Matter and R-Parity Violation*, JHEP **1401** (2014) 075, `arXiv:1309.4462 [hep-ph]`.

[37] C. Csaki, Y. Grossman, and B. Heidenreich, *MFV SUSY: A Natural Theory for R-Parity Violation*, Phys. Rev. D **85** (2012) 095009, `arXiv:1111.1239 [hep-ph]`.

[38] Y. Bai, A. Katz, and B. Tweedie, *Pulling Out All the Stops: Searching for RPV SUSY with Stop-Jets*, JHEP **1401** (2014) 040, `arXiv:1309.6631 [hep-ph]`.

[39] ALEPH Collaboration, A. Heister et al., *Search for supersymmetric particles with R parity violating decays in e^+e^- collisions at $\sqrt{s}$ up to 209-GeV*, Eur. Phys. J. C **31** (2003), `arXiv:hep-ex/0210014 [hep-ex]`.

[40] CDF Collaboration, T. Aaltonen et al., *Search for Pair Production of Strongly Interacting Particles Decaying to Pairs of Jets in $p\bar{p}$ Collisions at $\sqrt{s}$ = 1.96 TeV*, Phys. Rev. Lett. **111** (2013) 031802, `arXiv:1303.2699 [hep-ex]`.

[41] CMS Collaboration, *Search for pair-produced resonances decaying to jet pairs in proton-proton collisions at $\sqrt{s}$ = 8 TeV*, Phys. Lett. B **747** (2015) 98, `arXiv:1412.7706 [hep-ex]`.

[42] ATLAS Collaboration, *Search for new phenomena in final states with large jet multiplicities and missing transverse momentum at $\sqrt{s}$ = 8 TeV proton–proton collisions using the ATLAS experiment*, JHEP **1310** (2013) 130, `arXiv:1308.1841 [hep-ex]`.

[43] ATLAS Collaboration, *Search for supersymmetry at $\sqrt{s}$ = 8 TeV in final states with jets and two same-sign leptons or three leptons with the ATLAS detector*, JHEP **1406** (2014) 035, `arXiv:1404.2500 [hep-ex]`.

[44] R. Barbier et al., *R-parity violating supersymmetry*, Phys. Rept. **420** (2005) 1, `arXiv:hep-ph/0406039 [hep-ph]`.

[45] ATLAS Collaboration, *Jet mass and substructure of inclusive jets in $\sqrt{s}$ = 7 TeV pp collisions with the ATLAS experiment*, JHEP **1205** (2012) 128, `arXiv:1203.4606 [hep-ex]`.

[46] ATLAS Collaboration, *ATLAS measurements of the properties of jets for boosted particle searches*, Phys. Rev. D **86** (2012) 072006, `arXiv:1206.5369 [hep-ex]`.

[47] ATLAS Collaboration, *A search for $t\bar{t}$ resonances in lepton+jets events with highly boosted top quarks collected in pp collisions at $\sqrt{s}$ = 7 TeV with the ATLAS detector*, JHEP **1209** (2012) 041, `arXiv:1207.2409 [hep-ex]`.

[48] ATLAS Collaboration, *Performance of jet substructure techniques for large-R jets in proton–proton collisions at $\sqrt{s}$ = 7 TeV using the ATLAS detector*, JHEP **1309** (2013) 076, `arXiv:1306.4945 [hep-ex]`.

[49] ATLAS Collaboration, *Measurement of the cross-section of high transverse momentum vector bosons reconstructed as single jets and studies of jet substructure in pp collisions at $\sqrt{s}$ = 7 TeV with the ATLAS detector*, New J. Phys. **16** (2014) 113013, `arXiv:1407.0800 [hep-ex]`.

[50] ATLAS Collaboration, *The ATLAS Experiment at the CERN Large Hadron Collider*, JINST **3** (2008) S08003.

[51] ATLAS Collaboration, *Performance of the ATLAS Detector using First Collision Data*, JHEP **1009** (2010) 056, `arXiv:hep-ex/1005.5254 [hep-ex]`.

[52] ATLAS Collaboration, *Charged-particle multiplicities in pp interactions measured with the ATLAS detector at the LHC*, New J. Phys. **13** (2011) 053033, `arXiv:1012.5104 [hep-ex]`.

[53] ATLAS Collaboration, *Performance of the ATLAS Trigger System in 2010*, Eur. Phys. J. C **72** (2012) 1849, `arXiv:1110.1530 [hep-ex]`.

[54] GEANT4 Collaboration, S. Agostinelli et al., *GEANT4: A simulation toolkit*, Nucl. Instrum. Meth. A **506** (2003) 250.

[55] ATLAS Collaboration, *The ATLAS simulation infrastructure*, Eur. Phys. J. C **70** (2010) 823, `arXiv:1005.4568 [physics.ins-det]`.

[56] T. Sjöstrand, S. Mrenna, and P. Z. Skands, *A Brief Introduction to PYTHIA 8.1*, Comput. Phys. Commun. **178** (2008) 852, `arXiv:0710.3820 [hep-ph]`.

[57] ATLAS Collaboration, *Further ATLAS tunes of* PYTHIA *6 and Pythia 8*, ATL-PHYS-PUB-2011-014, 2011, `http://cds.cern.ch/record/1400677`.

[58] G. Watt and R. Thorne, *Study of Monte Carlo approach to experimental uncertainty propagation with MSTW 2008 PDFs*, JHEP **1208** (2012) 052, `arXiv:1205.4024 [hep-ph]`.

[59] M. Bähr et al., *Herwig++ physics and manual*, Eur. Phys. J. C **58** (2008) 639, `arXiv:0803.0883 [hep-ph]`.

[60] S. Gieseke, C. Röhr, and A. Siödmok, *Colour reconnections in Herwig++*, Eur. Phys. J. C **72** (2012) 2225, `arXiv:1206.0041 [hep-ph]`.

[61] J. Pumplin et al., *New generation of parton distributions with uncertainties from global QCD analysis*, JHEP **0207** (2002) 012, `arXiv:0201195 [hep-ph]`.

[62] P. M. Nadolsky et al., *Implications of CTEQ global analysis for collider observables*, Phys. Rev. D **78** (2008) 013004, `arXiv:0802.0007 [hep-ph]`.

[63] W. Beenakker, M. Krämer, T. Plehn, M. Spira, and P. M. Zerwas, *Stop production at hadron colliders*, Nucl. Phys. B **515** (1998) 3, `arXiv:hep-ph/9710451 [hep-ph]`.

[64] W. Beenakker et al., *Supersymmetric top and bottom squark production at hadron colliders*, JHEP **1008** (2010) 098, `arXiv:1006.4771 [hep-ph]`.

[65] W. Beenakker et al., *Squark and gluino hadroproduction*, Int. J. Mod. Phys. A **26** (2011) 2637, `arXiv:1105.1110 [hep-ph]`.

[66] M. Krämer et al., *Supersymmetry production cross sections in pp collisions at $\sqrt{s}$ = 7 TeV*, `arXiv:1206.2892 [hep-ph]`.

[67] J. Alwall, M. Herquet, F. Maltoni, O. Mattelaer, and T. Stelzer, *MadGraph 5 : Going Beyond*, JHEP **1106** (2011) 128, `arXiv:1106.0522 [hep-ph]`.

[68] ATLAS Collaboration, *ATLAS tunes of* PYTHIA *6 and Pythia 8 for MC11*, ATL-PHYS-PUB-2011-009, 2011, `http://cds.cern.ch/record/1363300`.

[69] P. Nason, *A New method for combining NLO QCD with shower Monte Carlo algorithms*, JHEP **0411** (2004) 040, `arXiv:hep-ph/0409146 [hep-ph]`.

[70] S. Frixione, P. Nason, and C. Oleari, *Matching NLO QCD computations with Parton Shower simulations: the POWHEG method*, JHEP **0711** (2007) 070, `arXiv:0709.2092 [hep-ph]`.

[71] S. Alioli, P. Nason, C. Oleari, and E. Re, *A general framework for implementing NLO calculations in shower Monte Carlo programs: the POWHEG BOX*, JHEP **1006** (2010) 043, `arXiv:1002.2581 [hep-ph]`.

[72] H.-L. Lai et al., *New parton distributions for collider physics*, Phys. Rev. D **82** (2010) 074024, `arXiv:1007.2241 [hep-ph]`.

[73] P. Z. Skands, *Tuning Monte Carlo Generators: The Perugia Tunes*, Phys. Rev. D **82** (2010) 074018, `arXiv:1005.3457 [hep-ph]`.

[74] M. Czakon, P. Fiedler, and A. Mitov, *Total Top-Quark Pair-Production Cross Section at Hadron Colliders Through $O(\alpha_S^4)$*, Phys. Rev. Lett. **110** (2013) 252004, `arXiv:1303.6254 [hep-ph]`.

[75] M. Czakon and A. Mitov, *NNLO corrections to top pair production at hadron colliders: the quark-gluon reaction*, JHEP **1301** (2013) 080, `arXiv:1210.6832 [hep-ph]`.

[76] M. Czakon and A. Mitov, *NNLO corrections to top-pair production at hadron colliders: the all-fermionic scattering channels*, JHEP **1212** (2012) 054, `arXiv:1207.0236 [hep-ph]`.

[77] P. Bärnreuther, M. Czakon, and A. Mitov, *Percent Level Precision Physics at the Tevatron: First Genuine NNLO QCD Corrections to $q\bar{q} \to t\bar{t} + X$*, Phys. Rev. Lett. **109** (2012) 132001, `arXiv:1204.5201 [hep-ph]`.

[78] M. Cacciari, M. Czakon, M. Mangano, A. Mitov, and P. Nason, *Top-pair production at hadron colliders with next-to-next-to-leading logarithmic soft-gluon resummation*, Phys. Lett. B **710** (2012) 612–622, `arXiv:1111.5869 [hep-ph]`.

[79] M. Czakon and A. Mitov, *Top++: A Program for the Calculation of the Top-Pair Cross-Section at Hadron Colliders*, Comput. Phys. Commun. **185** (2014) 2930, `arXiv:1112.5675 [hep-ph]`.

[80] M. Cacciari, G. P. Salam, and G. Soyez, *The anti-k_t jet clustering algorithm*, JHEP **0804** (2008) 063, `arXiv:0802.1189 [hep-ph]`.

[81] M. Cacciari, G. P. Salam, and G. Soyez, *FastJet User Manual*, Eur. Phys. J. C **72** (2012) 1896, `arXiv:1111.6097 [hep-ph]`.

[82] W. Lampl et al., *Calorimeter clustering algorithms: description and performance*, ATL-LARG-PUB-2008-002, 2008, `http://cdsweb.cern.ch/record/1099735`.

[83] ATLAS Collaboration, *Jet energy measurement and its systematic uncertainty in proton–proton collisions at $\sqrt{s}$ = 7 TeV with the ATLAS detector*, Eur. Phys. J. C **75** (2015) 17, `arXiv:1406.0076 [hep-ex]`.

[84] M. Cacciari and G. P. Salam, *Pileup subtraction using jet areas*, Phys. Lett. B **659** (2008) 119, arXiv:0707.1378 [hep-ph].

[85] ATLAS Collaboration, *Characterisation and mitigation of beam-induced backgrounds observed in the ATLAS detector during the 2011 proton–proton run*, JINST **8** (2013) P07004, arXiv:1303.0223 [hep-ex].

[86] ATLAS Collaboration, *Monitoring and data quality assessment of the ATLAS liquid argon calorimeter*, JINST **9** (2014) P07024, arXiv:1405.3768 [hep-ex].

[87] ATLAS Collaboration, *Performance of b-Jet Identification in the ATLAS Experiment*, Submitted to JINST (2015), arXiv:1512.01094 [hep-ex].

[88] B. Nachman, P. Nef, A. Schwartzman, M. Swiatlowski, and C. Wanotayaroj, *Jets from Jets: Re-clustering as a tool for large radius jet reconstruction and grooming at the LHC*, JHEP **1502** (2015) 075, arXiv:1407.2922 [hep-ph].

[89] Y. L. Dokshitzer, G. D. Leder, S. Moretti, and B. R. Webber, *Better jet clustering algorithms*, JHEP **9708** (1997) 001, arXiv:hep-ph/9707323 [hep-ph].

[90] M. Wobisch and T. Wengler, *Hadronization corrections to jet cross-sections in deep inelastic scattering*, in *Monte Carlo generators for HERA physics. Proceedings, Workshop, Hamburg, Germany, 1998-1999*. 1998. arXiv:hep-ph/9907280 [hep-ph].

[91] M. Son, C. Spethmann, and B. Tweedie, *Diboson-Jets and the Search for Resonant Zh Production*, JHEP **1208** (2012) 160, arXiv:1204.0525 [hep-ph].

[92] J. M. Butterworth et al., *Jet substructure as a new Higgs search channel at the LHC*, Phys. Rev. Lett. **100** (2008) 242001, arXiv:0802.2470 [hep-ph].

[93] ATLAS Collaboration, *Search for Massive Colored Scalars in Four-Jet Final States in $\sqrt{s} = 7$ TeV proton-proton collisions with the ATLAS Detector*, Eur. Phys. J. C **71** (2011) 1828, arXiv:1110.2693 [hep-ex].

[94] S. Schumann, A. Renaud, and D. Zerwas, *Hadronically decaying color-adjoint scalars at the LHC*, JHEP **1109** (2011) 074, arXiv:1108.2957 [hep-ph].

[95] S. Frixione and B. R. Webber, *Matching NLO QCD computations and parton shower simulations*, JHEP **0206** (2002) 029, arXiv:hep-ph/0204244 [hep-ph].

[96] G. Corcella et al., *HERWIG 6: An Event generator for hadron emission reactions with interfering gluons (including supersymmetric processes)*, JHEP **0101** (2001) 010, arXiv:hep-ph/0011363 [hep-ph].

[97] ATLAS Collaboration, *Improved luminosity determination in pp collisions at $\sqrt{s} = 7$ TeV using the ATLAS detector at the LHC*, Eur. Phys. J. C **73** (2013) 2518, arXiv:1302.4393 [hep-ex].

[98] A. L. Read, *Presentation of search results: The CL_s technique*, J. Phys. G **28** (2002) 2693.

[99] G. Cowan, K. Cranmer, E. Gross, and O. Vitells, *Asymptotic formulae for likelihood-based tests of new physics*, Eur. Phys. J. **C71** (2011) 1554, arXiv:1007.1727 [physics.data-an], [Erratum: Eur. Phys. J. C73, 2501 (2013)].

[100] M. Baak et al., *HistFitter software framework for statistical data analysis*, Eur. Phys. J. C **75** (2015) 153, arXiv:1410.1280 [hep-ex].

The ATLAS Collaboration

G. Aad[85], B. Abbott[112], J. Abdallah[150], O. Abdinov[11], B. Abeloos[116], R. Aben[106], M. Abolins[90], O.S. AbouZeid[157], H. Abramowicz[152], H. Abreu[151], R. Abreu[115], Y. Abulaiti[145a,145b], B.S. Acharya[163a,163b,a], L. Adamczyk[38a], D.L. Adams[25], J. Adelman[107], S. Adomeit[99], T. Adye[130], A.A. Affolder[74], T. Agatonovic-Jovin[13], J. Agricola[54], J.A. Aguilar-Saavedra[125a,125f], S.P. Ahlen[22], F. Ahmadov[65,b], G. Aielli[132a,132b], H. Akerstedt[145a,145b], T.P.A. Åkesson[81], A.V. Akimov[95], G.L. Alberghi[20a,20b], J. Albert[168], S. Albrand[55], M.J. Alconada Verzini[71], M. Aleksa[30], I.N. Aleksandrov[65], C. Alexa[26b], G. Alexander[152], T. Alexopoulos[10], M. Alhroob[112], G. Alimonti[91a], L. Alio[85], J. Alison[31], S.P. Alkire[35], B.M.M. Allbrooke[148], B.W. Allen[115], P.P. Allport[18], A. Aloisio[103a,103b], A. Alonso[36], F. Alonso[71], C. Alpigiani[137], B. Alvarez Gonzalez[30], D. Álvarez Piqueras[166], M.G. Alviggi[103a,103b], B.T. Amadio[15], K. Amako[66], Y. Amaral Coutinho[24a], C. Amelung[23], D. Amidei[89], S.P. Amor Dos Santos[125a,125c], A. Amorim[125a,125b], S. Amoroso[30], N. Amram[152], G. Amundsen[23], C. Anastopoulos[138], L.S. Ancu[49], N. Andari[107], T. Andeen[31], C.F. Anders[58b], G. Anders[30], J.K. Anders[74], K.J. Anderson[31], A. Andreazza[91a,91b], V. Andrei[58a], S. Angelidakis[9], I. Angelozzi[106], P. Anger[44], A. Angerami[35], F. Anghinolfi[30], A.V. Anisenkov[108,c], N. Anjos[12], A. Annovi[123a,123b], M. Antonelli[47], A. Antonov[97], J. Antos[143b], F. Anulli[131a], M. Aoki[66], L. Aperio Bella[18], G. Arabidze[90], Y. Arai[66], J.P. Araque[125a], A.T.H. Arce[45], F.A. Arduh[71], J-F. Arguin[94], S. Argyropoulos[63], M. Arik[19a], A.J. Armbruster[30], O. Arnaez[30], H. Arnold[48], M. Arratia[28], O. Arslan[21], A. Artamonov[96], G. Artoni[119], S. Artz[83], S. Asai[154], N. Asbah[42], A. Ashkenazi[152], B. Åsman[145a,145b], L. Asquith[148], K. Assamagan[25], R. Astalos[143a], M. Atkinson[164], N.B. Atlay[140], K. Augsten[127], G. Avolio[30], B. Axen[15], M.K. Ayoub[116], G. Azuelos[94,d], M.A. Baak[30], A.E. Baas[58a], M.J. Baca[18], H. Bachacou[135], K. Bachas[153], M. Backes[30], M. Backhaus[30], P. Bagiacchi[131a,131b], P. Bagnaia[131a,131b], Y. Bai[33a], J.T. Baines[130], O.K. Baker[175], E.M. Baldin[108,c], P. Balek[128], T. Balestri[147], F. Balli[84], W.K. Balunas[121], E. Banas[39], Sw. Banerjee[172,e], A.A.E. Bannoura[174], L. Barak[30], E.L. Barberio[88], D. Barberis[50a,50b], M. Barbero[85], T. Barillari[100], M. Barisonzi[163a,163b], T. Barklow[142], N. Barlow[28], S.L. Barnes[84], B.M. Barnett[130], R.M. Barnett[15], Z. Barnovska[5], A. Baroncelli[133a], G. Barone[23], A.J. Barr[119], L. Barranco Navarro[166], F. Barreiro[82], J. Barreiro Guimarães da Costa[33a], R. Bartoldus[142], A.E. Barton[72], P. Bartos[143a], A. Basalaev[122], A. Bassalat[116], A. Basye[164], R.L. Bates[53], S.J. Batista[157], J.R. Batley[28], M. Battaglia[136], M. Bauce[131a,131b], F. Bauer[135], H.S. Bawa[142,f], J.B. Beacham[110], M.D. Beattie[72], T. Beau[80], P.H. Beauchemin[160], R. Beccherle[123a,123b], P. Bechtle[21], H.P. Beck[17,g], K. Becker[119], M. Becker[83], M. Beckingham[169], C. Becot[116], A.J. Beddall[19b], A. Beddall[19b], V.A. Bednyakov[65], M. Bedognetti[106], C.P. Bee[147], L.J. Beemster[106], T.A. Beermann[30], M. Begel[25], J.K. Behr[119], C. Belanger-Champagne[87], W.H. Bell[49], G. Bella[152], L. Bellagamba[20a], A. Bellerive[29], M. Bellomo[86], K. Belotskiy[97], O. Beltramello[30], O. Benary[152], D. Benchekroun[134a], M. Bender[99], K. Bendtz[145a,145b], N. Benekos[10], Y. Benhammou[152], E. Benhar Noccioli[175], J.A. Benitez Garcia[158b], D.P. Benjamin[45], J.R. Bensinger[23], S. Bentvelsen[106], L. Beresford[119], M. Beretta[47], D. Berge[106], E. Bergeaas Kuutmann[165], N. Berger[5], F. Berghaus[168], J. Beringer[15], C. Bernard[22], N.R. Bernard[86], C. Bernius[109], F.U. Bernlochner[21], T. Berry[77], P. Berta[128], C. Bertella[83], G. Bertoli[145a,145b], F. Bertolucci[123a,123b], C. Bertsche[112], D. Bertsche[112], G.J. Besjes[36], O. Bessidskaia Bylund[145a,145b], M. Bessner[42], N. Besson[135], C. Betancourt[48], S. Bethke[100], A.J. Bevan[76], W. Bhimji[15], R.M. Bianchi[124], L. Bianchini[23], M. Bianco[30], O. Biebel[99], D. Biedermann[16], N.V. Biesuz[123a,123b], M. Biglietti[133a], J. Bilbao De Mendizabal[49], H. Bilokon[47], M. Bindi[54], S. Binet[116], A. Bingul[19b], C. Bini[131a,131b], S. Biondi[20a,20b], D.M. Bjergaard[45], C.W. Black[149], J.E. Black[142], K.M. Black[22], D. Blackburn[137], R.E. Blair[6], J.-B. Blanchard[135], J.E. Blanco[77], T. Blazek[143a], I. Bloch[42], C. Blocker[23], W. Blum[83,*], U. Blumenschein[54], S. Blunier[32a], G.J. Bobbink[106], V.S. Bobrovnikov[108,c], S.S. Bocchetta[81], A. Bocci[45],

C. Bock[99], M. Boehler[48], D. Boerner[174], J.A. Bogaerts[30], D. Bogavac[13], A.G. Bogdanchikov[108],
C. Bohm[145a], V. Boisvert[77], T. Bold[38a], V. Boldea[26b], A.S. Boldyrev[98], M. Bomben[80], M. Bona[76],
M. Boonekamp[135], A. Borisov[129], G. Borissov[72], J. Bortfeldt[99], V. Bortolotto[60a,60b,60c], K. Bos[106],
D. Boscherini[20a], M. Bosman[12], J. Boudreau[124], J. Bouffard[2], E.V. Bouhova-Thacker[72],
D. Boumediene[34], C. Bourdarios[116], N. Bousson[113], S.K. Boutle[53], A. Boveia[30], J. Boyd[30],
I.R. Boyko[65], J. Bracinik[18], A. Brandt[8], G. Brandt[54], O. Brandt[58a], U. Bratzler[155], B. Brau[86],
J.E. Brau[115], H.M. Braun[174,*], W.D. Breaden Madden[53], K. Brendlinger[121], A.J. Brennan[88],
L. Brenner[106], R. Brenner[165], S. Bressler[171], T.M. Bristow[46], D. Britton[53], D. Britzger[42], F.M. Brochu[28],
I. Brock[21], R. Brock[90], G. Brooijmans[35], T. Brooks[77], W.K. Brooks[32b], J. Brosamer[15], E. Brost[115],
P.A. Bruckman de Renstrom[39], D. Bruncko[143b], R. Bruneliere[48], A. Bruni[20a], G. Bruni[20a], BH Brunt[28],
M. Bruschi[20a], N. Bruscino[21], P. Bryant[31], L. Bryngemark[81], T. Buanes[14], Q. Buat[141], P. Buchholz[140],
A.G. Buckley[53], I.A. Budagov[65], F. Buehrer[48], L. Bugge[118], M.K. Bugge[118], O. Bulekov[97], D. Bullock[8],
H. Burckhart[30], S. Burdin[74], C.D. Burgard[48], B. Burghgrave[107], S. Burke[130], I. Burmeister[43],
E. Busato[34], D. Büscher[48], V. Büscher[83], P. Bussey[53], J.M. Butler[22], A.I. Butt[3], C.M. Buttar[53],
J.M. Butterworth[78], P. Butti[106], W. Buttinger[25], A. Buzatu[53], A.R. Buzykaev[108,c], S. Cabrera Urbán[166],
D. Caforio[127], V.M. Cairo[37a,37b], O. Cakir[4a], N. Calace[49], P. Calafiura[15], A. Calandri[85], G. Calderini[80],
P. Calfayan[99], L.P. Caloba[24a], D. Calvet[34], S. Calvet[34], T.P. Calvet[85], R. Camacho Toro[31], S. Camarda[42],
P. Camarri[132a,132b], D. Cameron[118], R. Caminal Armadans[164], C. Camincher[55], S. Campana[30],
M. Campanelli[78], A. Campoverde[147], V. Canale[103a,103b], A. Canepa[158a], M. Cano Bret[33e], J. Cantero[82],
R. Cantrill[125a], T. Cao[40], M.D.M. Capeans Garrido[30], I. Caprini[26b], M. Caprini[26b], M. Capua[37a,37b],
R. Caputo[83], R.M. Carbone[35], R. Cardarelli[132a], F. Cardillo[48], T. Carli[30], G. Carlino[103a],
L. Carminati[91a,91b], S. Caron[105], E. Carquin[32a], G.D. Carrillo-Montoya[30], J.R. Carter[28],
J. Carvalho[125a,125c], D. Casadei[78], M.P. Casado[12], M. Casolino[12], D.W. Casper[162],
E. Castaneda-Miranda[144a], A. Castelli[106], V. Castillo Gimenez[166], N.F. Castro[125a,h], A. Catinaccio[30],
J.R. Catmore[118], A. Cattai[30], J. Caudron[83], V. Cavaliere[164], D. Cavalli[91a], M. Cavalli-Sforza[12],
V. Cavasinni[123a,123b], F. Ceradini[133a,133b], L. Cerda Alberich[166], B.C. Cerio[45], A.S. Cerqueira[24b],
A. Cerri[148], L. Cerrito[76], F. Cerutti[15], M. Cerv[30], A. Cervelli[17], S.A. Cetin[19c], A. Chafaq[134a],
D. Chakraborty[107], I. Chalupkova[128], Y.L. Chan[60a], P. Chang[164], J.D. Chapman[28], D.G. Charlton[18],
C.C. Chau[157], C.A. Chavez Barajas[148], S. Che[110], S. Cheatham[72], A. Chegwidden[90], S. Chekanov[6],
S.V. Chekulaev[158a], G.A. Chelkov[65,i], M.A. Chelstowska[89], C. Chen[64], H. Chen[25], K. Chen[147],
S. Chen[33c], S. Chen[154], X. Chen[33f], Y. Chen[67], H.C. Cheng[89], Y. Cheng[31], A. Cheplakov[65],
E. Cheremushkina[129], R. Cherkaoui El Moursli[134e], V. Chernyatin[25,*], E. Cheu[7], L. Chevalier[135],
V. Chiarella[47], G. Chiarelli[123a,123b], G. Chiodini[73a], A.S. Chisholm[18], R.T. Chislett[78], A. Chitan[26b],
M.V. Chizhov[65], K. Choi[61], S. Chouridou[9], B.K.B. Chow[99], V. Christodoulou[78],
D. Chromek-Burckhart[30], J. Chudoba[126], A.J. Chuinard[87], J.J. Chwastowski[39], L. Chytka[114],
G. Ciapetti[131a,131b], A.K. Ciftci[4a], D. Cinca[53], V. Cindro[75], I.A. Cioara[21], A. Ciocio[15], F. Cirotto[103a,103b],
Z.H. Citron[171], M. Ciubancan[26b], A. Clark[49], B.L. Clark[57], P.J. Clark[46], R.N. Clarke[15],
C. Clement[145a,145b], Y. Coadou[85], M. Cobal[163a,163c], A. Coccaro[49], J. Cochran[64], L. Coffey[23],
L. Colasurdo[105], B. Cole[35], S. Cole[107], A.P. Colijn[106], J. Collot[55], T. Colombo[58c], G. Compostella[100],
P. Conde Muiño[125a,125b], E. Coniavitis[48], S.H. Connell[144b], I.A. Connelly[77], V. Consorti[48],
S. Constantinescu[26b], C. Conta[120a,120b], G. Conti[30], F. Conventi[103a,j], M. Cooke[15], B.D. Cooper[78],
A.M. Cooper-Sarkar[119], T. Cornelissen[174], M. Corradi[131a,131b], F. Corriveau[87,k], A. Corso-Radu[162],
A. Cortes-Gonzalez[12], G. Cortiana[100], G. Costa[91a], M.J. Costa[166], D. Costanzo[138], G. Cottin[28],
G. Cowan[77], B.E. Cox[84], K. Cranmer[109], S.J. Crawley[53], G. Cree[29], S. Crépé-Renaudin[55], F. Crescioli[80],
W.A. Cribbs[145a,145b], M. Crispin Ortuzar[119], M. Cristinziani[21], V. Croft[105], G. Crosetti[37a,37b],
T. Cuhadar Donszelmann[138], J. Cummings[175], M. Curatolo[47], J. Cúth[83], C. Cuthbert[149], H. Czirr[140],
P. Czodrowski[3], S. D'Auria[53], M. D'Onofrio[74], M.J. Da Cunha Sargedas De Sousa[125a,125b], C. Da Via[84],

W. Dabrowski[38a], A. Dafinca[119], T. Dai[89], O. Dale[14], F. Dallaire[94], C. Dallapiccola[86], M. Dam[36],
J.R. Dandoy[31], N.P. Dang[48], A.C. Daniells[18], M. Danninger[167], M. Dano Hoffmann[135], V. Dao[48],
G. Darbo[50a], S. Darmora[8], J. Dassoulas[3], A. Dattagupta[61], W. Davey[21], C. David[168], T. Davidek[128],
E. Davies[119,l], M. Davies[152], P. Davison[78], Y. Davygora[58a], E. Dawe[88], I. Dawson[138],
R.K. Daya-Ishmukhametova[86], K. De[8], R. de Asmundis[103a], A. De Benedetti[112], S. De Castro[20a,20b],
S. De Cecco[80], N. De Groot[105], P. de Jong[106], H. De la Torre[82], F. De Lorenzi[64], D. De Pedis[131a],
A. De Salvo[131a], U. De Sanctis[148], A. De Santo[148], J.B. De Vivie De Regie[116], W.J. Dearnaley[72],
R. Debbe[25], C. Debenedetti[136], D.V. Dedovich[65], I. Deigaard[106], J. Del Peso[82], T. Del Prete[123a,123b],
D. Delgove[116], F. Deliot[135], C.M. Delitzsch[49], M. Deliyergiyev[75], A. Dell'Acqua[30], L. Dell'Asta[22],
M. Dell'Orso[123a,123b], M. Della Pietra[103a,j], D. della Volpe[49], M. Delmastro[5], P.A. Delsart[55],
C. Deluca[106], D.A. DeMarco[157], S. Demers[175], M. Demichev[65], A. Demilly[80], S.P. Denisov[129],
D. Denysiuk[135], D. Derendarz[39], J.E. Derkaoui[134d], F. Derue[80], P. Dervan[74], K. Desch[21], C. Deterre[42],
K. Dette[43], P.O. Deviveiros[30], A. Dewhurst[130], S. Dhaliwal[23], A. Di Ciaccio[132a,132b], L. Di Ciaccio[5],
A. Di Domenico[131a,131b], C. Di Donato[131a,131b], A. Di Girolamo[30], B. Di Girolamo[30], A. Di Mattia[151],
B. Di Micco[133a,133b], R. Di Nardo[47], A. Di Simone[48], R. Di Sipio[157], D. Di Valentino[29], C. Diaconu[85],
M. Diamond[157], F.A. Dias[46], M.A. Diaz[32a], E.B. Diehl[89], J. Dietrich[16], S. Diglio[85], A. Dimitrievska[13],
J. Dingfelder[21], P. Dita[26b], S. Dita[26b], F. Dittus[30], F. Djama[85], T. Djobava[51b], J.I. Djuvsland[58a],
M.A.B. do Vale[24c], D. Dobos[30], M. Dobre[26b], C. Doglioni[81], T. Dohmae[154], J. Dolejsi[128], Z. Dolezal[128],
B.A. Dolgoshein[97,*], M. Donadelli[24d], S. Donati[123a,123b], P. Dondero[120a,120b], J. Donini[34], J. Dopke[130],
A. Doria[103a], M.T. Dova[71], A.T. Doyle[53], E. Drechsler[54], M. Dris[10], Y. Du[33d], J. Duarte-Campderros[152],
E. Dubreuil[34], E. Duchovni[171], G. Duckeck[99], O.A. Ducu[26b,85], D. Duda[106], A. Dudarev[30], L. Duflot[116],
L. Duguid[77], M. Dührssen[30], M. Dunford[58a], H. Duran Yildiz[4a], M. Düren[52], A. Durglishvili[51b],
D. Duschinger[44], B. Dutta[42], M. Dyndal[38a], C. Eckardt[42], K.M. Ecker[100], R.C. Edgar[89], W. Edson[2],
N.C. Edwards[46], T. Eifert[30], G. Eigen[14], K. Einsweiler[15], T. Ekelof[165], M. El Kacimi[134c],
V. Ellajosyula[85], M. Ellert[165], S. Elles[5], F. Ellinghaus[174], A.A. Elliot[168], N. Ellis[30], J. Elmsheuser[99],
M. Elsing[30], D. Emeliyanov[130], Y. Enari[154], O.C. Endner[83], M. Endo[117], J. Erdmann[43], A. Ereditato[17],
G. Ernis[174], J. Ernst[2], M. Ernst[25], S. Errede[164], E. Ertel[83], M. Escalier[116], H. Esch[43], C. Escobar[124],
B. Esposito[47], A.I. Etienvre[135], E. Etzion[152], H. Evans[61], A. Ezhilov[122], L. Fabbri[20a,20b], G. Facini[31],
R.M. Fakhrutdinov[129], S. Falciano[131a], R.J. Falla[78], J. Faltova[128], Y. Fang[33a], M. Fanti[91a,91b], A. Farbin[8],
A. Farilla[133a], C. Farina[124], T. Farooque[12], S. Farrell[15], S.M. Farrington[169], P. Farthouat[30], F. Fassi[134e],
P. Fassnacht[30], D. Fassouliotis[9], M. Faucci Giannelli[77], A. Favareto[50a,50b], L. Fayard[116], O.L. Fedin[122,m],
W. Fedorko[167], S. Feigl[118], L. Feligioni[85], C. Feng[33d], E.J. Feng[30], H. Feng[89], A.B. Fenyuk[129],
L. Feremenga[8], P. Fernandez Martinez[166], S. Fernandez Perez[12], J. Ferrando[53], A. Ferrari[165],
P. Ferrari[106], R. Ferrari[120a], D.E. Ferreira de Lima[53], A. Ferrer[166], D. Ferrere[49], C. Ferretti[89],
A. Ferretto Parodi[50a,50b], F. Fiedler[83], A. Filipčič[75], M. Filipuzzi[42], F. Filthaut[105], M. Fincke-Keeler[168],
K.D. Finelli[149], M.C.N. Fiolhais[125a,125c], L. Fiorini[166], A. Firan[40], A. Fischer[2], C. Fischer[12],
J. Fischer[174], W.C. Fisher[90], N. Flaschel[42], I. Fleck[140], P. Fleischmann[89], G.T. Fletcher[138], G. Fletcher[76],
R.R.M. Fletcher[121], T. Flick[174], A. Floderus[81], L.R. Flores Castillo[60a], M.J. Flowerdew[100],
G.T. Forcolin[84], A. Formica[135], A. Forti[84], D. Fournier[116], H. Fox[72], S. Fracchia[12], P. Francavilla[80],
M. Franchini[20a,20b], D. Francis[30], L. Franconi[118], M. Franklin[57], M. Frate[162], M. Fraternali[120a,120b],
D. Freeborn[78], S.M. Fressard-Batraneanu[30], F. Friedrich[44], D. Froidevaux[30], J.A. Frost[119],
C. Fukunaga[155], E. Fullana Torregrosa[83], T. Fusayasu[101], J. Fuster[166], C. Gabaldon[55], O. Gabizon[174],
A. Gabrielli[20a,20b], A. Gabrielli[15], G.P. Gach[38a], S. Gadatsch[30], S. Gadomski[49], G. Gagliardi[50a,50b],
P. Gagnon[61], C. Galea[105], B. Galhardo[125a,125c], E.J. Gallas[119], B.J. Gallop[130], P. Gallus[127], G. Galster[36],
K.K. Gan[110], J. Gao[33b,85], Y. Gao[46], Y.S. Gao[142,f], F.M. Garay Walls[46], C. García[166],
J.E. García Navarro[166], M. Garcia-Sciveres[15], R.W. Gardner[31], N. Garelli[142], V. Garonne[118], C. Gatti[47],
A. Gaudiello[50a,50b], G. Gaudio[120a], B. Gaur[140], L. Gauthier[94], I.L. Gavrilenko[95], C. Gay[167],

G. Gaycken[21], E.N. Gazis[10], Z. Gecse[167], C.N.P. Gee[130], Ch. Geich-Gimbel[21], M.P. Geisler[58a],
C. Gemme[50a], M.H. Genest[55], C. Geng[33b,n], S. Gentile[131a,131b], S. George[77], D. Gerbaudo[162],
A. Gershon[152], S. Ghasemi[140], H. Ghazlane[134b], B. Giacobbe[20a], S. Giagu[131a,131b], P. Giannetti[123a,123b],
B. Gibbard[25], S.M. Gibson[77], M. Gignac[167], M. Gilchriese[15], T.P.S. Gillam[28], D. Gillberg[29], G. Gilles[34],
D.M. Gingrich[3,d], N. Giokaris[9], M.P. Giordani[163a,163c], F.M. Giorgi[20a], F.M. Giorgi[16], P.F. Giraud[135],
P. Giromini[57], D. Giugni[91a], C. Giuliani[100], M. Giulini[58a], B.K. Gjelsten[118], S. Gkaitatzis[153],
I. Gkialas[153], E.L. Gkougkousis[116], L.K. Gladilin[98], C. Glasman[82], J. Glatzer[30], P.C.F. Glaysher[46],
A. Glazov[42], M. Goblirsch-Kolb[100], J.R. Goddard[76], J. Godlewski[39], S. Goldfarb[89], T. Golling[49],
D. Golubkov[129], A. Gomes[125a,125b,125d], R. Gonçalo[125a], J. Goncalves Pinto Firmino Da Costa[135],
L. Gonella[21], S. González de la Hoz[166], G. Gonzalez Parra[12], S. Gonzalez-Sevilla[49], L. Goossens[30],
P.A. Gorbounov[96], H.A. Gordon[25], I. Gorelov[104], B. Gorini[30], E. Gorini[73a,73b], A. Gorišek[75],
E. Gornicki[39], A.T. Goshaw[45], C. Gössling[43], M.I. Gostkin[65], C.R. Goudet[116], D. Goujdami[134c],
A.G. Goussiou[137], N. Govender[144b], E. Gozani[151], L. Graber[54], I. Grabowska-Bold[38a], P.O.J. Gradin[165],
P. Grafström[20a,20b], J. Gramling[49], E. Gramstad[118], S. Grancagnolo[16], V. Gratchev[122], H.M. Gray[30],
E. Graziani[133a], Z.D. Greenwood[79,o], C. Grefe[21], K. Gregersen[78], I.M. Gregor[42], P. Grenier[142],
K. Grevtsov[5], J. Griffiths[8], A.A. Grillo[136], K. Grimm[72], S. Grinstein[12,p], Ph. Gris[34], J.-F. Grivaz[116],
S. Groh[83], J.P. Grohs[44], E. Gross[171], J. Grosse-Knetter[54], G.C. Grossi[79], Z.J. Grout[148], L. Guan[89],
J. Guenther[127], F. Guescini[49], D. Guest[162], O. Gueta[152], E. Guido[50a,50b], T. Guillemin[5], S. Guindon[2],
U. Gul[53], C. Gumpert[30], J. Guo[33e], Y. Guo[33b,n], S. Gupta[119], G. Gustavino[131a,131b], P. Gutierrez[112],
N.G. Gutierrez Ortiz[78], C. Gutschow[44], C. Guyot[135], C. Gwenlan[119], C.B. Gwilliam[74], A. Haas[109],
C. Haber[15], H.K. Hadavand[8], N. Haddad[134e], A. Hadef[85], P. Haefner[21], S. Hageböck[21], Z. Hajduk[39],
H. Hakobyan[176], M. Haleem[42], J. Haley[113], D. Hall[119], G. Halladjian[90], G.D. Hallewell[85],
K. Hamacher[174], P. Hamal[114], K. Hamano[168], A. Hamilton[144a], G.N. Hamity[138], P.G. Hamnett[42],
L. Han[33b], K. Hanagaki[66,q], K. Hanawa[154], M. Hance[136], B. Haney[121], P. Hanke[58a], R. Hanna[135],
J.B. Hansen[36], J.D. Hansen[36], M.C. Hansen[21], P.H. Hansen[36], K. Hara[159], A.S. Hard[172],
T. Harenberg[174], F. Hariri[116], S. Harkusha[92], R.D. Harrington[46], P.F. Harrison[169], F. Hartjes[106],
M. Hasegawa[67], Y. Hasegawa[139], A. Hasib[112], S. Hassani[135], S. Haug[17], R. Hauser[90], L. Hauswald[44],
M. Havranek[126], C.M. Hawkes[18], R.J. Hawkings[30], A.D. Hawkins[81], T. Hayashi[159], D. Hayden[90],
C.P. Hays[119], J.M. Hays[76], H.S. Hayward[74], S.J. Haywood[130], S.J. Head[18], T. Heck[83], V. Hedberg[81],
L. Heelan[8], S. Heim[121], T. Heim[15], B. Heinemann[15], L. Heinrich[109], J. Hejbal[126], L. Helary[22],
S. Hellman[145a,145b], C. Helsens[30], J. Henderson[119], R.C.W. Henderson[72], Y. Heng[172], S. Henkelmann[167],
A.M. Henriques Correia[30], S. Henrot-Versille[116], G.H. Herbert[16], Y. Hernández Jiménez[166], G. Herten[48],
R. Hertenberger[99], L. Hervas[30], G.G. Hesketh[78], N.P. Hessey[106], J.W. Hetherly[40], R. Hickling[76],
E. Higón-Rodriguez[166], E. Hill[168], J.C. Hill[28], K.H. Hiller[42], S.J. Hillier[18], I. Hinchliffe[15], E. Hines[121],
R.R. Hinman[15], M. Hirose[156], D. Hirschbuehl[174], J. Hobbs[147], N. Hod[106], M.C. Hodgkinson[138],
P. Hodgson[138], A. Hoecker[30], M.R. Hoeferkamp[104], F. Hoenig[99], M. Hohlfeld[83], D. Hohn[21],
T.R. Holmes[15], M. Homann[43], T.M. Hong[124], B.H. Hooberman[164], W.H. Hopkins[115], Y. Horii[102],
A.J. Horton[141], J-Y. Hostachy[55], S. Hou[150], A. Hoummada[134a], J. Howard[119], J. Howarth[42],
M. Hrabovsky[114], I. Hristova[16], J. Hrivnac[116], T. Hryn'ova[5], A. Hrynevich[93], C. Hsu[144c], P.J. Hsu[150,r],
S.-C. Hsu[137], D. Hu[35], Q. Hu[33b], Y. Huang[42], Z. Hubacek[127], F. Hubaut[85], F. Huegging[21],
T.B. Huffman[119], E.W. Hughes[35], G. Hughes[72], M. Huhtinen[30], T.A. Hülsing[83], N. Huseynov[65,b],
J. Huston[90], J. Huth[57], G. Iacobucci[49], G. Iakovidis[25], I. Ibragimov[140], L. Iconomidou-Fayard[116],
E. Ideal[175], Z. Idrissi[134e], P. Iengo[30], O. Igonkina[106], T. Iizawa[170], Y. Ikegami[66], M. Ikeno[66],
Y. Ilchenko[31,s], D. Iliadis[153], N. Ilic[142], T. Ince[100], G. Introzzi[120a,120b], P. Ioannou[9], M. Iodice[133a],
K. Iordanidou[35], V. Ippolito[57], A. Irles Quiles[166], C. Isaksson[165], M. Ishino[68], M. Ishitsuka[156],
R. Ishmukhametov[110], C. Issever[119], S. Istin[19a], J.M. Iturbe Ponce[84], R. Iuppa[132a,132b], J. Ivarsson[81],
W. Iwanski[39], H. Iwasaki[66], J.M. Izen[41], V. Izzo[103a], S. Jabbar[3], B. Jackson[121], M. Jackson[74],

P. Jackson[1], V. Jain[2], K.B. Jakobi[83], K. Jakobs[48], S. Jakobsen[30], T. Jakoubek[126], D.O. Jamin[113],
D.K. Jana[79], E. Jansen[78], R. Jansky[62], J. Janssen[21], M. Janus[54], G. Jarlskog[81], N. Javadov[65,b],
T. Javůrek[48], F. Jeanneau[135], L. Jeanty[15], J. Jejelava[51a,t], G.-Y. Jeng[149], D. Jennens[88], P. Jenni[48,u],
J. Jentzsch[43], C. Jeske[169], S. Jézéquel[5], H. Ji[172], J. Jia[147], H. Jiang[64], Y. Jiang[33b], S. Jiggins[78],
J. Jimenez Pena[166], S. Jin[33a], A. Jinaru[26b], O. Jinnouchi[156], P. Johansson[138], K.A. Johns[7],
W.J. Johnson[137], K. Jon-And[145a,145b], G. Jones[169], R.W.L. Jones[72], S. Jones[7], T.J. Jones[74],
J. Jongmanns[58a], P.M. Jorge[125a,125b], J. Jovicevic[158a], X. Ju[172], A. Juste Rozas[12,p], M.K. Köhler[171],
M. Kaci[166], A. Kaczmarska[39], M. Kado[116], H. Kagan[110], M. Kagan[142], S.J. Kahn[85], E. Kajomovitz[45],
C.W. Kalderon[119], A. Kaluza[83], S. Kama[40], A. Kamenshchikov[129], N. Kanaya[154], S. Kaneti[28],
V.A. Kantserov[97], J. Kanzaki[66], B. Kaplan[109], L.S. Kaplan[172], A. Kapliy[31], D. Kar[144c], K. Karakostas[10],
A. Karamaoun[3], N. Karastathis[10,106], M.J. Kareem[54], E. Karentzos[10], M. Karnevskiy[83], S.N. Karpov[65],
Z.M. Karpova[65], K. Karthik[109], V. Kartvelishvili[72], A.N. Karyukhin[129], K. Kasahara[159], L. Kashif[172],
R.D. Kass[110], A. Kastanas[14], Y. Kataoka[154], C. Kato[154], A. Katre[49], J. Katzy[42], K. Kawade[102],
K. Kawagoe[70], T. Kawamoto[154], G. Kawamura[54], S. Kazama[154], V.F. Kazanin[108,c], R. Keeler[168],
R. Kehoe[40], J.S. Keller[42], J.J. Kempster[77], H. Keoshkerian[84], O. Kepka[126], B.P. Kerševan[75],
S. Kersten[174], R.A. Keyes[87], F. Khalil-zada[11], H. Khandanyan[145a,145b], A. Khanov[113],
A.G. Kharlamov[108,c], T.J. Khoo[28], V. Khovanskiy[96], E. Khramov[65], J. Khubua[51b,v], S. Kido[67],
H.Y. Kim[8], S.H. Kim[159], Y.K. Kim[31], N. Kimura[153], O.M. Kind[16], B.T. King[74], M. King[166],
S.B. King[167], J. Kirk[130], A.E. Kiryunin[100], T. Kishimoto[67], D. Kisielewska[38a], F. Kiss[48], K. Kiuchi[159],
O. Kivernyk[135], E. Kladiva[143b], M.H. Klein[35], M. Klein[74], U. Klein[74], K. Kleinknecht[83],
P. Klimek[145a,145b], A. Klimentov[25], R. Klingenberg[43], J.A. Klinger[138], T. Klioutchnikova[30],
E.-E. Kluge[58a], P. Kluit[106], S. Kluth[100], J. Knapik[39], E. Kneringer[62], E.B.F.G. Knoops[85], A. Knue[53],
A. Kobayashi[154], D. Kobayashi[156], T. Kobayashi[154], M. Kobel[44], M. Kocian[142], P. Kodys[128], T. Koffas[29],
E. Koffeman[106], L.A. Kogan[119], S. Kohlmann[174], T. Kohriki[66], T. Koi[142], H. Kolanoski[16], M. Kolb[58b],
I. Koletsou[5], A.A. Komar[95,*], Y. Komori[154], T. Kondo[66], N. Kondrashova[42], K. Köneke[48],
A.C. König[105], T. Kono[66,w], R. Konoplich[109,x], N. Konstantinidis[78], R. Kopeliansky[61], S. Koperny[38a],
L. Köpke[83], A.K. Kopp[48], K. Korcyl[39], K. Kordas[153], A. Korn[78], A.A. Korol[108,c], I. Korolkov[12],
E.V. Korolkova[138], O. Kortner[100], S. Kortner[100], T. Kosek[128], V.V. Kostyukhin[21], V.M. Kotov[65],
A. Kotwal[45], A. Kourkoumeli-Charalampidi[153], C. Kourkoumelis[9], V. Kouskoura[25], A. Koutsman[158a],
R. Kowalewski[168], T.Z. Kowalski[38a], W. Kozanecki[135], A.S. Kozhin[129], V.A. Kramarenko[98],
G. Kramberger[75], D. Krasnopevtsev[97], M.W. Krasny[80], A. Krasznahorkay[30], J.K. Kraus[21],
A. Kravchenko[25], M. Kretz[58c], J. Kretzschmar[74], K. Kreutzfeldt[52], P. Krieger[157], K. Krizka[31],
K. Kroeninger[43], H. Kroha[100], J. Kroll[121], J. Kroseberg[21], J. Krstic[13], U. Kruchonak[65], H. Krüger[21],
N. Krumnack[64], A. Kruse[172], M.C. Kruse[45], M. Kruskal[22], T. Kubota[88], H. Kucuk[78], S. Kuday[4b],
J.T. Kuechler[174], S. Kuehn[48], A. Kugel[58c], F. Kuger[173], A. Kuhl[136], T. Kuhl[42], V. Kukhtin[65],
R. Kukla[135], Y. Kulchitsky[92], S. Kuleshov[32b], M. Kuna[131a,131b], T. Kunigo[68], A. Kupco[126],
H. Kurashige[67], Y.A. Kurochkin[92], V. Kus[126], E.S. Kuwertz[168], M. Kuze[156], J. Kvita[114], T. Kwan[168],
D. Kyriazopoulos[138], A. La Rosa[100], J.L. La Rosa Navarro[24d], L. La Rotonda[37a,37b], C. Lacasta[166],
F. Lacava[131a,131b], J. Lacey[29], H. Lacker[16], D. Lacour[80], V.R. Lacuesta[166], E. Ladygin[65], R. Lafaye[5],
B. Laforge[80], T. Lagouri[175], S. Lai[54], L. Lambourne[78], S. Lammers[61], C.L. Lampen[7], W. Lampl[7],
E. Lançon[135], U. Landgraf[48], M.P.J. Landon[76], V.S. Lang[58a], J.C. Lange[12], A.J. Lankford[162], F. Lanni[25],
K. Lantzsch[21], A. Lanza[120a], S. Laplace[80], C. Lapoire[30], J.F. Laporte[135], T. Lari[91a],
F. Lasagni Manghi[20a,20b], M. Lassnig[30], P. Laurelli[47], W. Lavrijsen[15], A.T. Law[136], P. Laycock[74],
T. Lazovich[57], O. Le Dortz[80], E. Le Guirriec[85], E. Le Menedeu[12], M. LeBlanc[168], T. LeCompte[6],
F. Ledroit-Guillon[55], C.A. Lee[25], S.C. Lee[150], L. Lee[1], G. Lefebvre[80], M. Lefebvre[168], F. Legger[99],
C. Leggett[15], A. Lehan[74], G. Lehmann Miotto[30], X. Lei[7], W.A. Leight[29], A. Leisos[153,y], A.G. Leister[175],
M.A.L. Leite[24d], R. Leitner[128], D. Lellouch[171], B. Lemmer[54], K.J.C. Leney[78], T. Lenz[21], B. Lenzi[30],

R. Leone[7], S. Leone[123a,123b], C. Leonidopoulos[46], S. Leontsinis[10], C. Leroy[94], C.G. Lester[28],
M. Levchenko[122], J. Levêque[5], D. Levin[89], L.J. Levinson[171], M. Levy[18], A. Lewis[119], A.M. Leyko[21],
M. Leyton[41], B. Li[33b,z], H. Li[147], H.L. Li[31], L. Li[45], L. Li[33e], S. Li[45], X. Li[84], Y. Li[33c,aa], Z. Liang[136],
H. Liao[34], B. Liberti[132a], A. Liblong[157], P. Lichard[30], K. Lie[164], J. Liebal[21], W. Liebig[14], C. Limbach[21],
A. Limosani[149], S.C. Lin[150,ab], T.H. Lin[83], B.E. Lindquist[147], E. Lipeles[121], A. Lipniacka[14],
M. Lisovyi[58b], T.M. Liss[164], D. Lissauer[25], A. Lister[167], A.M. Litke[136], B. Liu[150,ac], D. Liu[150], H. Liu[89],
H. Liu[25], J. Liu[85], J.B. Liu[33b], K. Liu[85], L. Liu[164], M. Liu[45], M. Liu[33b], Y.L. Liu[33b], Y. Liu[33b],
M. Livan[120a,120b], A. Lleres[55], J. Llorente Merino[82], S.L. Lloyd[76], F. Lo Sterzo[150], E. Lobodzinska[42],
P. Loch[7], W.S. Lockman[136], F.K. Loebinger[84], A.E. Loevschall-Jensen[36], K.M. Loew[23], A. Loginov[175],
T. Lohse[16], K. Lohwasser[42], M. Lokajicek[126], B.A. Long[22], J.D. Long[164], R.E. Long[72], K.A. Looper[110],
L. Lopes[125a], D. Lopez Mateos[57], B. Lopez Paredes[138], I. Lopez Paz[12], A. Lopez Solis[80], J. Lorenz[99],
N. Lorenzo Martinez[61], M. Losada[161], P.J. Lösel[99], X. Lou[33a], A. Lounis[116], J. Love[6], P.A. Love[72],
H. Lu[60a], N. Lu[89], H.J. Lubatti[137], C. Luci[131a,131b], A. Lucotte[55], C. Luedtke[48], F. Luehring[61],
W. Lukas[62], L. Luminari[131a], O. Lundberg[145a,145b], B. Lund-Jensen[146], D. Lynn[25], R. Lysak[126],
E. Lytken[81], H. Ma[25], L.L. Ma[33d], G. Maccarrone[47], A. Macchiolo[100], C.M. Macdonald[138], B. Maček[75],
J. Machado Miguens[121,125b], D. Madaffari[85], R. Madar[34], H.J. Maddocks[165], W.F. Mader[44],
A. Madsen[42], J. Maeda[67], S. Maeland[14], T. Maeno[25], A. Maevskiy[98], E. Magradze[54], J. Mahlstedt[106],
C. Maiani[116], C. Maidantchik[24a], A.A. Maier[100], T. Maier[99], A. Maio[125a,125b,125d], S. Majewski[115],
Y. Makida[66], N. Makovec[116], B. Malaescu[80], Pa. Malecki[39], V.P. Maleev[122], F. Malek[55], U. Mallik[63],
D. Malon[6], C. Malone[142], S. Maltezos[10], V.M. Malyshev[108], S. Malyukov[30], J. Mamuzic[42],
G. Mancini[47], B. Mandelli[30], L. Mandelli[91a], I. Mandić[75], J. Maneira[125a,125b],
L. Manhaes de Andrade Filho[24b], J. Manjarres Ramos[158b], A. Mann[99], B. Mansoulie[135], R. Mantifel[87],
M. Mantoani[54], S. Manzoni[91a,91b], L. Mapelli[30], L. March[49], G. Marchiori[80], M. Marcisovsky[126],
M. Marjanovic[13], D.E. Marley[89], F. Marroquim[24a], S.P. Marsden[84], Z. Marshall[15], L.F. Marti[17],
S. Marti-Garcia[166], B. Martin[90], T.A. Martin[169], V.J. Martin[46], B. Martin dit Latour[14], M. Martinez[12,p],
S. Martin-Haugh[130], V.S. Martoiu[26b], A.C. Martyniuk[78], M. Marx[137], F. Marzano[131a], A. Marzin[30],
L. Masetti[83], T. Mashimo[154], R. Mashinistov[95], J. Masik[84], A.L. Maslennikov[108,c], I. Massa[20a,20b],
L. Massa[20a,20b], P. Mastrandrea[5], A. Mastroberardino[37a,37b], T. Masubuchi[154], P. Mättig[174],
J. Mattmann[83], J. Maurer[26b], S.J. Maxfield[74], D.A. Maximov[108,c], R. Mazini[150], S.M. Mazza[91a,91b],
N.C. Mc Fadden[104], G. Mc Goldrick[157], S.P. Mc Kee[89], A. McCarn[89], R.L. McCarthy[147],
T.G. McCarthy[29], K.W. McFarlane[56,*], J.A. Mcfayden[78], G. Mchedlidze[54], S.J. McMahon[130],
R.A. McPherson[168,k], M. Medinnis[42], S. Meehan[137], S. Mehlhase[99], A. Mehta[74], K. Meier[58a],
C. Meineck[99], B. Meirose[41], B.R. Mellado Garcia[144c], F. Meloni[17], A. Mengarelli[20a,20b], S. Menke[100],
E. Meoni[160], K.M. Mercurio[57], S. Mergelmeyer[16], P. Mermod[49], L. Merola[103a,103b], C. Meroni[91a],
F.S. Merritt[31], A. Messina[131a,131b], J. Metcalfe[6], A.S. Mete[162], C. Meyer[83], C. Meyer[121], J-P. Meyer[135],
J. Meyer[106], H. Meyer Zu Theenhausen[58a], R.P. Middleton[130], S. Miglioranzi[163a,163c], L. Mijović[21],
G. Mikenberg[171], M. Mikestikova[126], M. Mikuž[75], M. Milesi[88], A. Milic[30], D.W. Miller[31], C. Mills[46],
A. Milov[171], D.A. Milstead[145a,145b], A.A. Minaenko[129], Y. Minami[154], I.A. Minashvili[65], A.I. Mincer[109],
B. Mindur[38a], M. Mineev[65], Y. Ming[172], L.M. Mir[12], K.P. Mistry[121], T. Mitani[170], J. Mitrevski[99],
V.A. Mitsou[166], A. Miucci[49], P.S. Miyagawa[138], J.U. Mjörnmark[81], T. Moa[145a,145b], K. Mochizuki[85],
S. Mohapatra[35], W. Mohr[48], S. Molander[145a,145b], R. Moles-Valls[21], R. Monden[68], M.C. Mondragon[90],
K. Mönig[42], J. Monk[36], E. Monnier[85], A. Montalbano[147], J. Montejo Berlingen[30], F. Monticelli[71],
S. Monzani[91a,91b], R.W. Moore[3], N. Morange[116], D. Moreno[161], M. Moreno Llácer[54], P. Morettini[50a],
D. Mori[141], T. Mori[154], M. Morii[57], M. Morinaga[154], V. Morisbak[118], S. Moritz[83], A.K. Morley[149],
G. Mornacchi[30], J.D. Morris[76], S.S. Mortensen[36], L. Morvaj[147], M. Mosidze[51b], J. Moss[142],
K. Motohashi[156], R. Mount[142], E. Mountricha[25], S.V. Mouraviev[95,*], E.J.W. Moyse[86], S. Muanza[85],
R.D. Mudd[18], F. Mueller[100], J. Mueller[124], R.S.P. Mueller[99], T. Mueller[28], D. Muenstermann[72],

36

P. Mullen[53], G.A. Mullier[17], F.J. Munoz Sanchez[84], J.A. Murillo Quijada[18], W.J. Murray[169,130],
H. Musheghyan[54], A.G. Myagkov[129,ad], M. Myska[127], B.P. Nachman[142], O. Nackenhorst[49], J. Nadal[54],
K. Nagai[119], R. Nagai[66], Y. Nagai[85], K. Nagano[66], Y. Nagasaka[59], K. Nagata[159], M. Nagel[100],
E. Nagy[85], A.M. Nairz[30], Y. Nakahama[30], K. Nakamura[66], T. Nakamura[154], I. Nakano[111],
H. Namasivayam[41], R.F. Naranjo Garcia[42], R. Narayan[31], D.I. Narrias Villar[58a], I. Naryshkin[122],
T. Naumann[42], G. Navarro[161], R. Nayyar[7], H.A. Neal[89], P.Yu. Nechaeva[95], T.J. Neep[84], P.D. Nef[142],
A. Negri[120a,120b], M. Negrini[20a], S. Nektarijevic[105], C. Nellist[116], A. Nelson[162], S. Nemecek[126],
P. Nemethy[109], A.A. Nepomuceno[24a], M. Nessi[30,ae], M.S. Neubauer[164], M. Neumann[174],
R.M. Neves[109], P. Nevski[25], P.R. Newman[18], D.H. Nguyen[6], R.B. Nickerson[119], R. Nicolaidou[135],
B. Nicquevert[30], J. Nielsen[136], A. Nikiforov[16], V. Nikolaenko[129,ad], I. Nikolic-Audit[80],
K. Nikolopoulos[18], J.K. Nilsen[118], P. Nilsson[25], Y. Ninomiya[154], A. Nisati[131a], R. Nisius[100], T. Nobe[154],
L. Nodulman[6], M. Nomachi[117], I. Nomidis[29], T. Nooney[76], S. Norberg[112], M. Nordberg[30],
O. Novgorodova[44], S. Nowak[100], M. Nozaki[66], L. Nozka[114], K. Ntekas[10], E. Nurse[78], F. Nuti[88],
F. O'grady[7], D.C. O'Neil[141], V. O'Shea[53], F.G. Oakham[29,d], H. Oberlack[100], T. Obermann[21],
J. Ocariz[80], A. Ochi[67], I. Ochoa[35], J.P. Ochoa-Ricoux[32a], S. Oda[70], S. Odaka[66], H. Ogren[61], A. Oh[84],
S.H. Oh[45], C.C. Ohm[15], H. Ohman[165], H. Oide[30], H. Okawa[159], Y. Okumura[31], T. Okuyama[66],
A. Olariu[26b], L.F. Oleiro Seabra[125a], S.A. Olivares Pino[46], D. Oliveira Damazio[25], M.J.R. Olsson[31],
A. Olszewski[39], J. Olszowska[39], A. Onofre[125a,125e], K. Onogi[102], P.U.E. Onyisi[31,s], C.J. Oram[158a],
M.J. Oreglia[31], Y. Oren[152], D. Orestano[133a,133b], N. Orlando[153], R.S. Orr[157], B. Osculati[50a,50b],
R. Ospanov[84], G. Otero y Garzon[27], H. Otono[70], M. Ouchrif[134d], F. Ould-Saada[118], A. Ouraou[135],
K.P. Oussoren[106], Q. Ouyang[33a], A. Ovcharova[15], M. Owen[53], R.E. Owen[18], V.E. Ozcan[19a], N. Ozturk[8],
K. Pachal[141], A. Pacheco Pages[12], C. Padilla Aranda[12], M. Pagáčová[48], S. Pagan Griso[15], F. Paige[25],
P. Pais[86], K. Pajchel[118], G. Palacino[158b], S. Palestini[30], M. Palka[38b], D. Pallin[34], A. Palma[125a,125b],
E.St. Panagiotopoulou[10], C.E. Pandini[80], J.G. Panduro Vazquez[77], P. Pani[145a,145b], S. Panitkin[25],
D. Pantea[26b], L. Paolozzi[49], Th.D. Papadopoulou[10], K. Papageorgiou[153], A. Paramonov[6],
D. Paredes Hernandez[175], M.A. Parker[28], K.A. Parker[138], F. Parodi[50a,50b], J.A. Parsons[35], U. Parzefall[48],
V. Pascuzzi[157], E. Pasqualucci[131a], S. Passaggio[50a], F. Pastore[133a,133b,*], Fr. Pastore[77], G. Pásztor[29],
S. Pataraia[174], N.D. Patel[149], J.R. Pater[84], T. Pauly[30], J. Pearce[168], B. Pearson[112], L.E. Pedersen[36],
M. Pedersen[118], S. Pedraza Lopez[166], R. Pedro[125a,125b], S.V. Peleganchuk[108,c], D. Pelikan[165], O. Penc[126],
C. Peng[33a], H. Peng[33b], B. Penning[31], J. Penwell[61], D.V. Perepelitsa[25], E. Perez Codina[158a],
L. Perini[91a,91b], H. Pernegger[30], S. Perrella[103a,103b], R. Peschke[42], V.D. Peshekhonov[65], K. Peters[30],
R.F.Y. Peters[84], B.A. Petersen[30], T.C. Petersen[36], E. Petit[55], A. Petridis[1], C. Petridou[153], P. Petroff[116],
E. Petrolo[131a], F. Petrucci[133a,133b], N.E. Pettersson[156], A. Peyaud[135], R. Pezoa[32b], P.W. Phillips[130],
G. Piacquadio[142], E. Pianori[169], A. Picazio[86], E. Piccaro[76], M. Piccinini[20a,20b], M.A. Pickering[119],
R. Piegaia[27], J.E. Pilcher[31], A.D. Pilkington[84], A.W.J. Pin[84], J. Pina[125a,125b,125d],
M. Pinamonti[163a,163c,af], J.L. Pinfold[3], A. Pingel[36], S. Pires[80], H. Pirumov[42], M. Pitt[171], L. Plazak[143a],
M.-A. Pleier[25], V. Pleskot[83], E. Plotnikova[65], P. Plucinski[145a,145b], D. Pluth[64], R. Poettgen[145a,145b],
L. Poggioli[116], D. Pohl[21], G. Polesello[120a], A. Poley[42], A. Policicchio[37a,37b], R. Polifka[157], A. Polini[20a],
C.S. Pollard[53], V. Polychronakos[25], K. Pommès[30], L. Pontecorvo[131a], B.G. Pope[90], G.A. Popeneciu[26c],
D.S. Popovic[13], A. Poppleton[30], S. Pospisil[127], K. Potamianos[15], I.N. Potrap[65], C.J. Potter[28],
C.T. Potter[115], G. Poulard[30], J. Poveda[30], V. Pozdnyakov[65], M.E. Pozo Astigarraga[30], P. Pralavorio[85],
A. Pranko[15], S. Prell[64], D. Price[84], L.E. Price[6], M. Primavera[73a], S. Prince[87], M. Proissl[46],
K. Prokofiev[60c], F. Prokoshin[32b], E. Protopapadaki[135], S. Protopopescu[25], J. Proudfoot[6],
M. Przybycien[38a], D. Puddu[133a,133b], D. Puldon[147], M. Purohit[25,ag], P. Puzo[116], J. Qian[89], G. Qin[53],
Y. Qin[84], A. Quadt[54], D.R. Quarrie[15], W.B. Quayle[163a,163b], M. Queitsch-Maitland[84], D. Quilty[53],
S. Raddum[118], V. Radeka[25], V. Radescu[42], S.K. Radhakrishnan[147], P. Radloff[115], P. Rados[88],
F. Ragusa[91a,91b], G. Rahal[177], S. Rajagopalan[25], M. Rammensee[30], C. Rangel-Smith[165], F. Rauscher[99],

S. Rave[83], T. Ravenscroft[53], M. Raymond[30], A.L. Read[118], N.P. Readioff[74], D.M. Rebuzzi[120a,120b],
A. Redelbach[173], G. Redlinger[25], R. Reece[136], K. Reeves[41], L. Rehnisch[16], J. Reichert[121], H. Reisin[27],
C. Rembser[30], H. Ren[33a], M. Rescigno[131a], S. Resconi[91a], O.L. Rezanova[108,c], P. Reznicek[128],
R. Rezvani[94], R. Richter[100], S. Richter[78], E. Richter-Was[38b], O. Ricken[21], M. Ridel[80], P. Rieck[16],
C.J. Riegel[174], J. Rieger[54], O. Rifki[112], M. Rijssenbeek[147], A. Rimoldi[120a,120b], L. Rinaldi[20a], B. Ristić[49],
E. Ritsch[30], I. Riu[12], F. Rizatdinova[113], E. Rizvi[76], S.H. Robertson[87,k], A. Robichaud-Veronneau[87],
D. Robinson[28], J.E.M. Robinson[42], A. Robson[53], C. Roda[123a,123b], Y. Rodina[85], A. Rodriguez Perez[12],
S. Roe[30], C.S. Rogan[57], O. Røhne[118], A. Romaniouk[97], M. Romano[20a,20b], S.M. Romano Saez[34],
E. Romero Adam[166], N. Rompotis[137], M. Ronzani[48], L. Roos[80], E. Ros[166], S. Rosati[131a], K. Rosbach[48],
P. Rose[136], O. Rosenthal[140], V. Rossetti[145a,145b], E. Rossi[103a,103b], L.P. Rossi[50a], J.H.N. Rosten[28],
R. Rosten[137], M. Rotaru[26b], I. Roth[171], J. Rothberg[137], D. Rousseau[116], C.R. Royon[135], A. Rozanov[85],
Y. Rozen[151], X. Ruan[144c], F. Rubbo[142], I. Rubinskiy[42], V.I. Rud[98], M.S. Rudolph[157], F. Rühr[48],
A. Ruiz-Martinez[30], Z. Rurikova[48], N.A. Rusakovich[65], A. Ruschke[99], H.L. Russell[137],
J.P. Rutherfoord[7], N. Ruthmann[30], Y.F. Ryabov[122], M. Rybar[164], G. Rybkin[116], N.C. Ryder[119],
A. Ryzhov[129], A.F. Saavedra[149], G. Sabato[106], S. Sacerdoti[27], H.F-W. Sadrozinski[136], R. Sadykov[65],
F. Safai Tehrani[131a], P. Saha[107], M. Sahinsoy[58a], M. Saimpert[135], T. Saito[154], H. Sakamoto[154],
Y. Sakurai[170], G. Salamanna[133a,133b], A. Salamon[132a], J.E. Salazar Loyola[32b], D. Salek[106],
P.H. Sales De Bruin[137], D. Salihagic[100], A. Salnikov[142], J. Salt[166], D. Salvatore[37a,37b], F. Salvatore[148],
A. Salvucci[60a], A. Salzburger[30], D. Sammel[48], D. Sampsonidis[153], A. Sanchez[103a,103b], J. Sánchez[166],
V. Sanchez Martinez[166], H. Sandaker[118], R.L. Sandbach[76], H.G. Sander[83], M.P. Sanders[99],
M. Sandhoff[174], C. Sandoval[161], R. Sandstroem[100], D.P.C. Sankey[130], M. Sannino[50a,50b], A. Sansoni[47],
C. Santoni[34], R. Santonico[132a,132b], H. Santos[125a], I. Santoyo Castillo[148], K. Sapp[124], A. Sapronov[65],
J.G. Saraiva[125a,125d], B. Sarrazin[21], O. Sasaki[66], Y. Sasaki[154], K. Sato[159], G. Sauvage[5,*], E. Sauvan[5],
G. Savage[77], P. Savard[157,d], C. Sawyer[130], L. Sawyer[79,o], J. Saxon[31], C. Sbarra[20a], A. Sbrizzi[20a,20b],
T. Scanlon[78], D.A. Scannicchio[162], M. Scarcella[149], V. Scarfone[37a,37b], J. Schaarschmidt[171],
P. Schacht[100], D. Schaefer[30], R. Schaefer[42], J. Schaeffer[83], S. Schaepe[21], S. Schaetzel[58b], U. Schäfer[83],
A.C. Schaffer[116], D. Schaile[99], R.D. Schamberger[147], V. Scharf[58a], V.A. Schegelsky[122], D. Scheirich[128],
M. Schernau[162], C. Schiavi[50a,50b], C. Schillo[48], M. Schioppa[37a,37b], S. Schlenker[30], K. Schmieden[30],
C. Schmitt[83], S. Schmitt[58b], S. Schmitt[42], S. Schmitz[83], B. Schneider[158a], Y.J. Schnellbach[74],
U. Schnoor[48], L. Schoeffel[135], A. Schoening[58b], B.D. Schoenrock[90], E. Schopf[21],
A.L.S. Schorlemmer[54], M. Schott[83], D. Schouten[158a], J. Schovancova[8], S. Schramm[49], M. Schreyer[173],
N. Schuh[83], M.J. Schultens[21], H.-C. Schultz-Coulon[58a], H. Schulz[16], M. Schumacher[48],
B.A. Schumm[136], Ph. Schune[135], C. Schwanenberger[84], A. Schwartzman[142], T.A. Schwarz[89],
Ph. Schwegler[100], H. Schweiger[84], Ph. Schwemling[135], R. Schwienhorst[90], J. Schwindling[135],
T. Schwindt[21], G. Sciolla[23], F. Scuri[123a,123b], F. Scutti[88], J. Searcy[89], P. Seema[21], S.C. Seidel[104],
A. Seiden[136], F. Seifert[127], J.M. Seixas[24a], G. Sekhniaidze[103a], K. Sekhon[89], S.J. Sekula[40],
D.M. Seliverstov[122,*], N. Semprini-Cesari[20a,20b], C. Serfon[30], L. Serin[116], L. Serkin[163a,163b],
M. Sessa[133a,133b], R. Seuster[158a], H. Severini[112], T. Sfiligoj[75], F. Sforza[30], A. Sfyrla[49], E. Shabalina[54],
N.W. Shaikh[145a,145b], L.Y. Shan[33a], R. Shang[164], J.T. Shank[22], M. Shapiro[15], P.B. Shatalov[96],
K. Shaw[163a,163b], S.M. Shaw[84], A. Shcherbakova[145a,145b], C.Y. Shehu[148], P. Sherwood[78], L. Shi[150,ah],
S. Shimizu[67], C.O. Shimmin[162], M. Shimojima[101], M. Shiyakova[65], A. Shmeleva[95], D. Shoaleh Saadi[94],
M.J. Shochet[31], S. Shojaii[91a,91b], S. Shrestha[110], E. Shulga[97], M.A. Shupe[7], P. Sicho[126], P.E. Sidebo[146],
O. Sidiropoulou[173], D. Sidorov[113], A. Sidoti[20a,20b], F. Siegert[44], Dj. Sijacki[13], J. Silva[125a,125d],
S.B. Silverstein[145a], V. Simak[127], O. Simard[5], Lj. Simic[13], S. Simion[116], E. Simioni[83], B. Simmons[78],
D. Simon[34], M. Simon[83], P. Sinervo[157], N.B. Sinev[115], M. Sioli[20a,20b], G. Siragusa[173],
S.Yu. Sivoklokov[98], J. Sjölin[145a,145b], T.B. Sjursen[14], M.B. Skinner[72], H.P. Skottowe[57], P. Skubic[112],
M. Slater[18], T. Slavicek[127], M. Slawinska[106], K. Sliwa[160], V. Smakhtin[171], B.H. Smart[46], L. Smestad[14],

38

S.Yu. Smirnov[97], Y. Smirnov[97], L.N. Smirnova[98,ai], O. Smirnova[81], M.N.K. Smith[35], R.W. Smith[35],
M. Smizanska[72], K. Smolek[127], A.A. Snesarev[95], G. Snidero[76], S. Snyder[25], R. Sobie[168,k], F. Socher[44],
A. Soffer[152], D.A. Soh[150,ah], G. Sokhrannyi[75], C.A. Solans Sanchez[30], M. Solar[127], E.Yu. Soldatov[97],
U. Soldevila[166], A.A. Solodkov[129], A. Soloshenko[65], O.V. Solovyanov[129], V. Solovyev[122], P. Sommer[48],
H.Y. Song[33b,z], N. Soni[1], A. Sood[15], A. Sopczak[127], V. Sopko[127], V. Sorin[12], D. Sosa[58b],
C.L. Sotiropoulou[123a,123b], R. Soualah[163a,163c], A.M. Soukharev[108,c], D. South[42], B.C. Sowden[77],
S. Spagnolo[73a,73b], M. Spalla[123a,123b], M. Spangenberg[169], F. Spanò[77], D. Sperlich[16], F. Spettel[100],
R. Spighi[20a], G. Spigo[30], L.A. Spiller[88], M. Spousta[128], R.D. St. Denis[53,*], A. Stabile[91a], S. Staerz[30],
J. Stahlman[121], R. Stamen[58a], S. Stamm[16], E. Stanecka[39], R.W. Stanek[6], C. Stanescu[133a],
M. Stanescu-Bellu[42], M.M. Stanitzki[42], S. Stapnes[118], E.A. Starchenko[129], G.H. Stark[31], J. Stark[55],
P. Staroba[126], P. Starovoitov[58a], R. Staszewski[39], P. Steinberg[25], B. Stelzer[141], H.J. Stelzer[30],
O. Stelzer-Chilton[158a], H. Stenzel[52], G.A. Stewart[53], J.A. Stillings[21], M.C. Stockton[87], M. Stoebe[87],
G. Stoicea[26b], P. Stolte[54], S. Stonjek[100], A.R. Stradling[8], A. Straessner[44], M.E. Stramaglia[17],
J. Strandberg[146], S. Strandberg[145a,145b], A. Strandlie[118], M. Strauss[112], P. Strizenec[143b], R. Ströhmer[173],
D.M. Strom[115], R. Stroynowski[40], A. Strubig[105], S.A. Stucci[17], B. Stugu[14], N.A. Styles[42], D. Su[142],
J. Su[124], R. Subramaniam[79], S. Suchek[58a], Y. Sugaya[117], M. Suk[127], V.V. Sulin[95], S. Sultansoy[4c],
T. Sumida[68], S. Sun[57], X. Sun[33a], J.E. Sundermann[48], K. Suruliz[148], G. Susinno[37a,37b], M.R. Sutton[148],
S. Suzuki[66], M. Svatos[126], M. Swiatlowski[31], I. Sykora[143a], T. Sykora[128], D. Ta[48], C. Taccini[133a,133b],
K. Tackmann[42], J. Taenzer[157], A. Taffard[162], R. Tafirout[158a], N. Taiblum[152], H. Takai[25], R. Takashima[69],
H. Takeda[67], T. Takeshita[139], Y. Takubo[66], M. Talby[85], A.A. Talyshev[108,c], J.Y.C. Tam[173], K.G. Tan[88],
J. Tanaka[154], R. Tanaka[116], S. Tanaka[66], B.B. Tannenwald[110], S. Tapia Araya[32b], S. Tapprogge[83],
S. Tarem[151], G.F. Tartarelli[91a], P. Tas[128], M. Tasevsky[126], T. Tashiro[68], E. Tassi[37a,37b],
A. Tavares Delgado[125a,125b], Y. Tayalati[134d], A.C. Taylor[104], G.N. Taylor[88], P.T.E. Taylor[88],
W. Taylor[158b], F.A. Teischinger[30], P. Teixeira-Dias[77], K.K. Temming[48], D. Temple[141], H. Ten Kate[30],
P.K. Teng[150], J.J. Teoh[117], F. Tepel[174], S. Terada[66], K. Terashi[154], J. Terron[82], S. Terzo[100], M. Testa[47],
R.J. Teuscher[157,k], T. Theveneaux-Pelzer[85], J.P. Thomas[18], J. Thomas-Wilsker[77], E.N. Thompson[35],
P.D. Thompson[18], R.J. Thompson[84], A.S. Thompson[53], L.A. Thomsen[175], E. Thomson[121],
M. Thomson[28], M.J. Tibbetts[15], R.E. Ticse Torres[85], V.O. Tikhomirov[95,aj], Yu.A. Tikhonov[108,c],
S. Timoshenko[97], E. Tiouchichine[85], P. Tipton[175], S. Tisserant[85], K. Todome[156], T. Todorov[5,*],
S. Todorova-Nova[128], J. Tojo[70], S. Tokár[143a], K. Tokushuku[66], E. Tolley[57], L. Tomlinson[84],
M. Tomoto[102], L. Tompkins[142,ak], K. Toms[104], B. Tong[57], E. Torrence[115], H. Torres[141],
E. Torró Pastor[137], J. Toth[85,al], F. Touchard[85], D.R. Tovey[138], T. Trefzger[173], L. Tremblet[30], A. Tricoli[30],
I.M. Trigger[158a], S. Trincaz-Duvoid[80], M.F. Tripiana[12], W. Trischuk[157], B. Trocmé[55], A. Trofymov[42],
C. Troncon[91a], M. Trottier-McDonald[15], M. Trovatelli[168], L. Truong[163a,163c], M. Trzebinski[39],
A. Trzupek[39], J.C-L. Tseng[119], P.V. Tsiareshka[92], G. Tsipolitis[10], N. Tsirintanis[9], S. Tsiskaridze[12],
V. Tsiskaridze[48], E.G. Tskhadadze[51a], K.M. Tsui[60a], I.I. Tsukerman[96], V. Tsulaia[15], S. Tsuno[66],
D. Tsybychev[147], A. Tudorache[26b], V. Tudorache[26b], A.N. Tuna[57], S.A. Tupputi[20a,20b],
S. Turchikhin[98,ai], D. Turecek[127], D. Turgeman[171], R. Turra[91a,91b], A.J. Turvey[40], P.M. Tuts[35],
M. Tylmad[145a,145b], M. Tyndel[130], I. Ueda[154], R. Ueno[29], M. Ughetto[145a,145b], F. Ukegawa[159], G. Unal[30],
A. Undrus[25], G. Unel[162], F.C. Ungaro[88], Y. Unno[66], C. Unverdorben[99], J. Urban[143b], P. Urquijo[88],
P. Urrejola[83], G. Usai[8], A. Usanova[62], L. Vacavant[85], V. Vacek[127], B. Vachon[87], C. Valderanis[83],
N. Valencic[106], S. Valentinetti[20a,20b], A. Valero[166], L. Valery[12], S. Valkar[128], S. Vallecorsa[49],
J.A. Valls Ferrer[166], W. Van Den Wollenberg[106], P.C. Van Der Deijl[106], R. van der Geer[106],
H. van der Graaf[106], N. van Eldik[151], P. van Gemmeren[6], J. Van Nieuwkoop[141], I. van Vulpen[106],
M.C. van Woerden[30], M. Vanadia[131a,131b], W. Vandelli[30], R. Vanguri[121], A. Vaniachine[6],
G. Vardanyan[176], R. Vari[131a], E.W. Varnes[7], T. Varol[40], D. Varouchas[80], A. Vartapetian[8], K.E. Varvell[149],
F. Vazeille[34], T. Vazquez Schroeder[87], J. Veatch[7], L.M. Veloce[157], F. Veloso[125a,125c], S. Veneziano[131a],

A. Ventura[73a,73b], M. Venturi[168], N. Venturi[157], A. Venturini[23], V. Vercesi[120a], M. Verducci[131a,131b],
W. Verkerke[106], J.C. Vermeulen[106], A. Vest[44,am], M.C. Vetterli[141,d], O. Viazlo[81], I. Vichou[164],
T. Vickey[138], O.E. Vickey Boeriu[138], G.H.A. Viehhauser[119], S. Viel[15], R. Vigne[62], M. Villa[20a,20b],
M. Villaplana Perez[91a,91b], E. Vilucchi[47], M.G. Vincter[29], V.B. Vinogradov[65], I. Vivarelli[148],
S. Vlachos[10], D. Vladoiu[99], M. Vlasak[127], M. Vogel[32a], P. Vokac[127], G. Volpi[123a,123b], M. Volpi[88],
H. von der Schmitt[100], E. von Toerne[21], V. Vorobel[128], K. Vorobev[97], M. Vos[166], R. Voss[30],
J.H. Vossebeld[74], N. Vranjes[13], M. Vranjes Milosavljevic[13], V. Vrba[126], M. Vreeswijk[106],
R. Vuillermet[30], I. Vukotic[31], Z. Vykydal[127], P. Wagner[21], W. Wagner[174], H. Wahlberg[71],
S. Wahrmund[44], J. Wakabayashi[102], J. Walder[72], R. Walker[99], W. Walkowiak[140], V. Wallangen[145a,145b],
C. Wang[150], C. Wang[33d,85], F. Wang[172], H. Wang[15], H. Wang[40], J. Wang[42], J. Wang[149], K. Wang[87],
R. Wang[6], S.M. Wang[150], T. Wang[21], T. Wang[35], X. Wang[175], C. Wanotayaroj[115], A. Warburton[87],
C.P. Ward[28], D.R. Wardrope[78], A. Washbrook[46], P.M. Watkins[18], A.T. Watson[18], I.J. Watson[149],
M.F. Watson[18], G. Watts[137], S. Watts[84], B.M. Waugh[78], S. Webb[84], M.S. Weber[17], S.W. Weber[173],
J.S. Webster[6], A.R. Weidberg[119], B. Weinert[61], J. Weingarten[54], C. Weiser[48], H. Weits[106], P.S. Wells[30],
T. Wenaus[25], T. Wengler[30], S. Wenig[30], N. Wermes[21], M. Werner[48], P. Werner[30], M. Wessels[58a],
J. Wetter[160], K. Whalen[115], A.M. Wharton[72], A. White[8], M.J. White[1], R. White[32b], S. White[123a,123b],
D. Whiteson[162], F.J. Wickens[130], W. Wiedenmann[172], M. Wielers[130], P. Wienemann[21],
C. Wiglesworth[36], L.A.M. Wiik-Fuchs[21], A. Wildauer[100], H.G. Wilkens[30], H.H. Williams[121],
S. Williams[106], C. Willis[90], S. Willocq[86], J.A. Wilson[18], I. Wingerter-Seez[5], F. Winklmeier[115],
B.T. Winter[21], M. Wittgen[142], J. Wittkowski[99], S.J. Wollstadt[83], M.W. Wolter[39], H. Wolters[125a,125c],
B.K. Wosiek[39], J. Wotschack[30], M.J. Woudstra[84], K.W. Wozniak[39], M. Wu[55], M. Wu[31], S.L. Wu[172],
X. Wu[49], Y. Wu[89], T.R. Wyatt[84], B.M. Wynne[46], S. Xella[36], D. Xu[33a], L. Xu[25], B. Yabsley[149],
S. Yacoob[144a], R. Yakabe[67], D. Yamaguchi[156], Y. Yamaguchi[117], A. Yamamoto[66], S. Yamamoto[154],
T. Yamanaka[154], K. Yamauchi[102], Y. Yamazaki[67], Z. Yan[22], H. Yang[33e], H. Yang[172], Y. Yang[150],
Z. Yang[14], W-M. Yao[15], Y.C. Yap[80], Y. Yasu[66], E. Yatsenko[5], K.H. Yau Wong[21], J. Ye[40], S. Ye[25],
I. Yeletskikh[65], A.L. Yen[57], E. Yildirim[42], K. Yorita[170], R. Yoshida[6], K. Yoshihara[121], C. Young[142],
C.J.S. Young[30], S. Youssef[22], D.R. Yu[15], J. Yu[8], J.M. Yu[89], J. Yu[64], L. Yuan[67], S.P.Y. Yuen[21],
I. Yusuff[28,an], B. Zabinski[39], R. Zaidan[33d], A.M. Zaitsev[129,ad], N. Zakharchuk[42], J. Zalieckas[14],
A. Zaman[147], S. Zambito[57], L. Zanello[131a,131b], D. Zanzi[88], C. Zeitnitz[174], M. Zeman[127], A. Zemla[38a],
J.C. Zeng[164], Q. Zeng[142], K. Zengel[23], O. Zenin[129], T. Ženiš[143a], D. Zerwas[116], D. Zhang[89], F. Zhang[172],
G. Zhang[33b,z], H. Zhang[33c], J. Zhang[6], L. Zhang[48], R. Zhang[21], R. Zhang[33b,ao], X. Zhang[33d],
Z. Zhang[116], X. Zhao[40], Y. Zhao[33d,116], Z. Zhao[33b], A. Zhemchugov[65], J. Zhong[119], B. Zhou[89],
C. Zhou[45], L. Zhou[35], L. Zhou[40], M. Zhou[147], N. Zhou[33f], C.G. Zhu[33d], H. Zhu[33a], J. Zhu[89], Y. Zhu[33b],
X. Zhuang[33a], K. Zhukov[95], A. Zibell[173], D. Zieminska[61], N.I. Zimine[65], C. Zimmermann[83],
S. Zimmermann[48], Z. Zinonos[54], M. Zinser[83], M. Ziolkowski[140], L. Živković[13], G. Zobernig[172],
A. Zoccoli[20a,20b], M. zur Nedden[16], G. Zurzolo[103a,103b], L. Zwalinski[30].

1 Department of Physics, University of Adelaide, Adelaide, Australia
2 Physics Department, SUNY Albany, Albany NY, United States of America
3 Department of Physics, University of Alberta, Edmonton AB, Canada
4 (a) Department of Physics, Ankara University, Ankara; (b) Istanbul Aydin University, Istanbul; (c) Division of Physics, TOBB University of Economics and Technology, Ankara, Turkey
5 LAPP, CNRS/IN2P3 and Université Savoie Mont Blanc, Annecy-le-Vieux, France
6 High Energy Physics Division, Argonne National Laboratory, Argonne IL, United States of America
7 Department of Physics, University of Arizona, Tucson AZ, United States of America
8 Department of Physics, The University of Texas at Arlington, Arlington TX, United States of America
9 Physics Department, University of Athens, Athens, Greece

[10] Physics Department, National Technical University of Athens, Zografou, Greece

[11] Institute of Physics, Azerbaijan Academy of Sciences, Baku, Azerbaijan

[12] Institut de Física d'Altes Energies (IFAE), The Barcelona Institute of Science and Technology, Barcelona, Spain, Spain

[13] Institute of Physics, University of Belgrade, Belgrade, Serbia

[14] Department for Physics and Technology, University of Bergen, Bergen, Norway

[15] Physics Division, Lawrence Berkeley National Laboratory and University of California, Berkeley CA, United States of America

[16] Department of Physics, Humboldt University, Berlin, Germany

[17] Albert Einstein Center for Fundamental Physics and Laboratory for High Energy Physics, University of Bern, Bern, Switzerland

[18] School of Physics and Astronomy, University of Birmingham, Birmingham, United Kingdom

[19] [a] Department of Physics, Bogazici University, Istanbul; [b] Department of Physics Engineering, Gaziantep University, Gaziantep; [c] Department of Physics, Dogus University, Istanbul, Turkey

[20] [a] INFN Sezione di Bologna; [b] Dipartimento di Fisica e Astronomia, Università di Bologna, Bologna, Italy

[21] Physikalisches Institut, University of Bonn, Bonn, Germany

[22] Department of Physics, Boston University, Boston MA, United States of America

[23] Department of Physics, Brandeis University, Waltham MA, United States of America

[24] [a] Universidade Federal do Rio De Janeiro COPPE/EE/IF, Rio de Janeiro; [b] Electrical Circuits Department, Federal University of Juiz de Fora (UFJF), Juiz de Fora; [c] Federal University of Sao Joao del Rei (UFSJ), Sao Joao del Rei; [d] Instituto de Fisica, Universidade de Sao Paulo, Sao Paulo, Brazil

[25] Physics Department, Brookhaven National Laboratory, Upton NY, United States of America

[26] [a] Transilvania University of Brasov, Brasov, Romania; [b] National Institute of Physics and Nuclear Engineering, Bucharest; [c] National Institute for Research and Development of Isotopic and Molecular Technologies, Physics Department, Cluj Napoca; [d] University Politehnica Bucharest, Bucharest; [e] West University in Timisoara, Timisoara, Romania

[27] Departamento de Física, Universidad de Buenos Aires, Buenos Aires, Argentina

[28] Cavendish Laboratory, University of Cambridge, Cambridge, United Kingdom

[29] Department of Physics, Carleton University, Ottawa ON, Canada

[30] CERN, Geneva, Switzerland

[31] Enrico Fermi Institute, University of Chicago, Chicago IL, United States of America

[32] [a] Departamento de Física, Pontificia Universidad Católica de Chile, Santiago; [b] Departamento de Física, Universidad Técnica Federico Santa María, Valparaíso, Chile

[33] [a] Institute of High Energy Physics, Chinese Academy of Sciences, Beijing; [b] Department of Modern Physics, University of Science and Technology of China, Anhui; [c] Department of Physics, Nanjing University, Jiangsu; [d] School of Physics, Shandong University, Shandong; [e] Department of Physics and Astronomy, Shanghai Key Laboratory for Particle Physics and Cosmology, Shanghai Jiao Tong University, Shanghai; [f] Physics Department, Tsinghua University, Beijing 100084, China

[34] Laboratoire de Physique Corpusculaire, Clermont Université and Université Blaise Pascal and CNRS/IN2P3, Clermont-Ferrand, France

[35] Nevis Laboratory, Columbia University, Irvington NY, United States of America

[36] Niels Bohr Institute, University of Copenhagen, Kobenhavn, Denmark

[37] [a] INFN Gruppo Collegato di Cosenza, Laboratori Nazionali di Frascati; [b] Dipartimento di Fisica, Università della Calabria, Rende, Italy

[38] [a] AGH University of Science and Technology, Faculty of Physics and Applied Computer Science, Krakow; [b] Marian Smoluchowski Institute of Physics, Jagiellonian University, Krakow, Poland

[39] Institute of Nuclear Physics Polish Academy of Sciences, Krakow, Poland

[40] Physics Department, Southern Methodist University, Dallas TX, United States of America

[41] Physics Department, University of Texas at Dallas, Richardson TX, United States of America

[42] DESY, Hamburg and Zeuthen, Germany

[43] Institut für Experimentelle Physik IV, Technische Universität Dortmund, Dortmund, Germany

[44] Institut für Kern- und Teilchenphysik, Technische Universität Dresden, Dresden, Germany

[45] Department of Physics, Duke University, Durham NC, United States of America

[46] SUPA - School of Physics and Astronomy, University of Edinburgh, Edinburgh, United Kingdom

[47] INFN Laboratori Nazionali di Frascati, Frascati, Italy

[48] Fakultät für Mathematik und Physik, Albert-Ludwigs-Universität, Freiburg, Germany

[49] Section de Physique, Université de Genève, Geneva, Switzerland

[50] [a] INFN Sezione di Genova; [b] Dipartimento di Fisica, Università di Genova, Genova, Italy

[51] [a] E. Andronikashvili Institute of Physics, Iv. Javakhishvili Tbilisi State University, Tbilisi; [b] High Energy Physics Institute, Tbilisi State University, Tbilisi, Georgia

[52] II Physikalisches Institut, Justus-Liebig-Universität Giessen, Giessen, Germany

[53] SUPA - School of Physics and Astronomy, University of Glasgow, Glasgow, United Kingdom

[54] II Physikalisches Institut, Georg-August-Universität, Göttingen, Germany

[55] Laboratoire de Physique Subatomique et de Cosmologie, Université Grenoble-Alpes, CNRS/IN2P3, Grenoble, France

[56] Department of Physics, Hampton University, Hampton VA, United States of America

[57] Laboratory for Particle Physics and Cosmology, Harvard University, Cambridge MA, United States of America

[58] [a] Kirchhoff-Institut für Physik, Ruprecht-Karls-Universität Heidelberg, Heidelberg; [b] Physikalisches Institut, Ruprecht-Karls-Universität Heidelberg, Heidelberg; [c] ZITI Institut für technische Informatik, Ruprecht-Karls-Universität Heidelberg, Mannheim, Germany

[59] Faculty of Applied Information Science, Hiroshima Institute of Technology, Hiroshima, Japan

[60] [a] Department of Physics, The Chinese University of Hong Kong, Shatin, N.T., Hong Kong; [b] Department of Physics, The University of Hong Kong, Hong Kong; [c] Department of Physics, The Hong Kong University of Science and Technology, Clear Water Bay, Kowloon, Hong Kong, China

[61] Department of Physics, Indiana University, Bloomington IN, United States of America

[62] Institut für Astro- und Teilchenphysik, Leopold-Franzens-Universität, Innsbruck, Austria

[63] University of Iowa, Iowa City IA, United States of America

[64] Department of Physics and Astronomy, Iowa State University, Ames IA, United States of America

[65] Joint Institute for Nuclear Research, JINR Dubna, Dubna, Russia

[66] KEK, High Energy Accelerator Research Organization, Tsukuba, Japan

[67] Graduate School of Science, Kobe University, Kobe, Japan

[68] Faculty of Science, Kyoto University, Kyoto, Japan

[69] Kyoto University of Education, Kyoto, Japan

[70] Department of Physics, Kyushu University, Fukuoka, Japan

[71] Instituto de Física La Plata, Universidad Nacional de La Plata and CONICET, La Plata, Argentina

[72] Physics Department, Lancaster University, Lancaster, United Kingdom

[73] [a] INFN Sezione di Lecce; [b] Dipartimento di Matematica e Fisica, Università del Salento, Lecce, Italy

[74] Oliver Lodge Laboratory, University of Liverpool, Liverpool, United Kingdom

[75] Department of Physics, Jožef Stefan Institute and University of Ljubljana, Ljubljana, Slovenia

[76] School of Physics and Astronomy, Queen Mary University of London, London, United Kingdom

[77] Department of Physics, Royal Holloway University of London, Surrey, United Kingdom

[78] Department of Physics and Astronomy, University College London, London, United Kingdom

[79] Louisiana Tech University, Ruston LA, United States of America

[80] Laboratoire de Physique Nucléaire et de Hautes Energies, UPMC and Université Paris-Diderot and CNRS/IN2P3, Paris, France

[81] Fysiska institutionen, Lunds universitet, Lund, Sweden

[82] Departamento de Fisica Teorica C-15, Universidad Autonoma de Madrid, Madrid, Spain

[83] Institut für Physik, Universität Mainz, Mainz, Germany

[84] School of Physics and Astronomy, University of Manchester, Manchester, United Kingdom

[85] CPPM, Aix-Marseille Université and CNRS/IN2P3, Marseille, France

[86] Department of Physics, University of Massachusetts, Amherst MA, United States of America

[87] Department of Physics, McGill University, Montreal QC, Canada

[88] School of Physics, University of Melbourne, Victoria, Australia

[89] Department of Physics, The University of Michigan, Ann Arbor MI, United States of America

[90] Department of Physics and Astronomy, Michigan State University, East Lansing MI, United States of America

[91] [a] INFN Sezione di Milano; [b] Dipartimento di Fisica, Università di Milano, Milano, Italy

[92] B.I. Stepanov Institute of Physics, National Academy of Sciences of Belarus, Minsk, Republic of Belarus

[93] National Scientific and Educational Centre for Particle and High Energy Physics, Minsk, Republic of Belarus

[94] Group of Particle Physics, University of Montreal, Montreal QC, Canada

[95] P.N. Lebedev Physical Institute of the Russian Academy of Sciences, Moscow, Russia

[96] Institute for Theoretical and Experimental Physics (ITEP), Moscow, Russia

[97] National Research Nuclear University MEPhI, Moscow, Russia

[98] D.V. Skobeltsyn Institute of Nuclear Physics, M.V. Lomonosov Moscow State University, Moscow, Russia

[99] Fakultät für Physik, Ludwig-Maximilians-Universität München, München, Germany

[100] Max-Planck-Institut für Physik (Werner-Heisenberg-Institut), München, Germany

[101] Nagasaki Institute of Applied Science, Nagasaki, Japan

[102] Graduate School of Science and Kobayashi-Maskawa Institute, Nagoya University, Nagoya, Japan

[103] [a] INFN Sezione di Napoli; [b] Dipartimento di Fisica, Università di Napoli, Napoli, Italy

[104] Department of Physics and Astronomy, University of New Mexico, Albuquerque NM, United States of America

[105] Institute for Mathematics, Astrophysics and Particle Physics, Radboud University Nijmegen/Nikhef, Nijmegen, Netherlands

[106] Nikhef National Institute for Subatomic Physics and University of Amsterdam, Amsterdam, Netherlands

[107] Department of Physics, Northern Illinois University, DeKalb IL, United States of America

[108] Budker Institute of Nuclear Physics, SB RAS, Novosibirsk, Russia

[109] Department of Physics, New York University, New York NY, United States of America

[110] Ohio State University, Columbus OH, United States of America

[111] Faculty of Science, Okayama University, Okayama, Japan

[112] Homer L. Dodge Department of Physics and Astronomy, University of Oklahoma, Norman OK, United States of America

[113] Department of Physics, Oklahoma State University, Stillwater OK, United States of America

[114] Palacký University, RCPTM, Olomouc, Czech Republic

[115] Center for High Energy Physics, University of Oregon, Eugene OR, United States of America

[116] LAL, Univ. Paris-Sud, CNRS/IN2P3, Université Paris-Saclay, Orsay, France

[117] Graduate School of Science, Osaka University, Osaka, Japan

[118] Department of Physics, University of Oslo, Oslo, Norway

[119] Department of Physics, Oxford University, Oxford, United Kingdom

[120] [a] INFN Sezione di Pavia; [b] Dipartimento di Fisica, Università di Pavia, Pavia, Italy

[121] Department of Physics, University of Pennsylvania, Philadelphia PA, United States of America

[122] National Research Centre "Kurchatov Institute" B.P.Konstantinov Petersburg Nuclear Physics Institute, St. Petersburg, Russia

[123] [a] INFN Sezione di Pisa; [b] Dipartimento di Fisica E. Fermi, Università di Pisa, Pisa, Italy

[124] Department of Physics and Astronomy, University of Pittsburgh, Pittsburgh PA, United States of America

[125] [a] Laboratório de Instrumentação e Física Experimental de Partículas - LIP, Lisboa; [b] Faculdade de Ciências, Universidade de Lisboa, Lisboa; [c] Department of Physics, University of Coimbra, Coimbra; [d] Centro de Física Nuclear da Universidade de Lisboa, Lisboa; [e] Departamento de Fisica, Universidade do Minho, Braga; [f] Departamento de Fisica Teorica y del Cosmos and CAFPE, Universidad de Granada, Granada (Spain); [g] Dep Fisica and CEFITEC of Faculdade de Ciencias e Tecnologia, Universidade Nova de Lisboa, Caparica, Portugal

[126] Institute of Physics, Academy of Sciences of the Czech Republic, Praha, Czech Republic

[127] Czech Technical University in Prague, Praha, Czech Republic

[128] Faculty of Mathematics and Physics, Charles University in Prague, Praha, Czech Republic

[129] State Research Center Institute for High Energy Physics (Protvino), NRC KI, Russia

[130] Particle Physics Department, Rutherford Appleton Laboratory, Didcot, United Kingdom

[131] [a] INFN Sezione di Roma; [b] Dipartimento di Fisica, Sapienza Università di Roma, Roma, Italy

[132] [a] INFN Sezione di Roma Tor Vergata; [b] Dipartimento di Fisica, Università di Roma Tor Vergata, Roma, Italy

[133] [a] INFN Sezione di Roma Tre; [b] Dipartimento di Matematica e Fisica, Università Roma Tre, Roma, Italy

[134] [a] Faculté des Sciences Ain Chock, Réseau Universitaire de Physique des Hautes Energies - Université Hassan II, Casablanca; [b] Centre National de l'Energie des Sciences Techniques Nucleaires, Rabat; [c] Faculté des Sciences Semlalia, Université Cadi Ayyad, LPHEA-Marrakech; [d] Faculté des Sciences, Université Mohamed Premier and LPTPM, Oujda; [e] Faculté des sciences, Université Mohammed V, Rabat, Morocco

[135] DSM/IRFU (Institut de Recherches sur les Lois Fondamentales de l'Univers), CEA Saclay (Commissariat à l'Energie Atomique et aux Energies Alternatives), Gif-sur-Yvette, France

[136] Santa Cruz Institute for Particle Physics, University of California Santa Cruz, Santa Cruz CA, United States of America

[137] Department of Physics, University of Washington, Seattle WA, United States of America

[138] Department of Physics and Astronomy, University of Sheffield, Sheffield, United Kingdom

[139] Department of Physics, Shinshu University, Nagano, Japan

[140] Fachbereich Physik, Universität Siegen, Siegen, Germany

[141] Department of Physics, Simon Fraser University, Burnaby BC, Canada

[142] SLAC National Accelerator Laboratory, Stanford CA, United States of America

[143] [a] Faculty of Mathematics, Physics & Informatics, Comenius University, Bratislava; [b] Department of Subnuclear Physics, Institute of Experimental Physics of the Slovak Academy of Sciences, Kosice, Slovak Republic

[144] [a] Department of Physics, University of Cape Town, Cape Town; [b] Department of Physics, University of Johannesburg, Johannesburg; [c] School of Physics, University of the Witwatersrand,

Johannesburg, South Africa

[145] (a) Department of Physics, Stockholm University; (b) The Oskar Klein Centre, Stockholm, Sweden

[146] Physics Department, Royal Institute of Technology, Stockholm, Sweden

[147] Departments of Physics & Astronomy and Chemistry, Stony Brook University, Stony Brook NY, United States of America

[148] Department of Physics and Astronomy, University of Sussex, Brighton, United Kingdom

[149] School of Physics, University of Sydney, Sydney, Australia

[150] Institute of Physics, Academia Sinica, Taipei, Taiwan

[151] Department of Physics, Technion: Israel Institute of Technology, Haifa, Israel

[152] Raymond and Beverly Sackler School of Physics and Astronomy, Tel Aviv University, Tel Aviv, Israel

[153] Department of Physics, Aristotle University of Thessaloniki, Thessaloniki, Greece

[154] International Center for Elementary Particle Physics and Department of Physics, The University of Tokyo, Tokyo, Japan

[155] Graduate School of Science and Technology, Tokyo Metropolitan University, Tokyo, Japan

[156] Department of Physics, Tokyo Institute of Technology, Tokyo, Japan

[157] Department of Physics, University of Toronto, Toronto ON, Canada

[158] (a) TRIUMF, Vancouver BC; (b) Department of Physics and Astronomy, York University, Toronto ON, Canada

[159] Faculty of Pure and Applied Sciences, and Center for Integrated Research in Fundamental Science and Engineering, University of Tsukuba, Tsukuba, Japan

[160] Department of Physics and Astronomy, Tufts University, Medford MA, United States of America

[161] Centro de Investigaciones, Universidad Antonio Narino, Bogota, Colombia

[162] Department of Physics and Astronomy, University of California Irvine, Irvine CA, United States of America

[163] (a) INFN Gruppo Collegato di Udine, Sezione di Trieste, Udine; (b) ICTP, Trieste; (c) Dipartimento di Chimica, Fisica e Ambiente, Università di Udine, Udine, Italy

[164] Department of Physics, University of Illinois, Urbana IL, United States of America

[165] Department of Physics and Astronomy, University of Uppsala, Uppsala, Sweden

[166] Instituto de Física Corpuscular (IFIC) and Departamento de Física Atómica, Molecular y Nuclear and Departamento de Ingeniería Electrónica and Instituto de Microelectrónica de Barcelona (IMB-CNM), University of Valencia and CSIC, Valencia, Spain

[167] Department of Physics, University of British Columbia, Vancouver BC, Canada

[168] Department of Physics and Astronomy, University of Victoria, Victoria BC, Canada

[169] Department of Physics, University of Warwick, Coventry, United Kingdom

[170] Waseda University, Tokyo, Japan

[171] Department of Particle Physics, The Weizmann Institute of Science, Rehovot, Israel

[172] Department of Physics, University of Wisconsin, Madison WI, United States of America

[173] Fakultät für Physik und Astronomie, Julius-Maximilians-Universität, Würzburg, Germany

[174] Fakult[a]t für Mathematik und Naturwissenschaften, Fachgruppe Physik, Bergische Universität Wuppertal, Wuppertal, Germany

[175] Department of Physics, Yale University, New Haven CT, United States of America

[176] Yerevan Physics Institute, Yerevan, Armenia

[177] Centre de Calcul de l'Institut National de Physique Nucléaire et de Physique des Particules (IN2P3), Villeurbanne, France

[a] Also at Department of Physics, King's College London, London, United Kingdom

[b] Also at Institute of Physics, Azerbaijan Academy of Sciences, Baku, Azerbaijan

^{c} Also at Novosibirsk State University, Novosibirsk, Russia

^{d} Also at TRIUMF, Vancouver BC, Canada

^{e} Also at Department of Physics & Astronomy, University of Louisville, Louisville, KY, United States of America

^{f} Also at Department of Physics, California State University, Fresno CA, United States of America

^{g} Also at Department of Physics, University of Fribourg, Fribourg, Switzerland

^{h} Also at Departamento de Fisica e Astronomia, Faculdade de Ciencias, Universidade do Porto, Portugal

^{i} Also at Tomsk State University, Tomsk, Russia

^{j} Also at Universita di Napoli Parthenope, Napoli, Italy

^{k} Also at Institute of Particle Physics (IPP), Canada

^{l} Also at Particle Physics Department, Rutherford Appleton Laboratory, Didcot, United Kingdom

^{m} Also at Department of Physics, St. Petersburg State Polytechnical University, St. Petersburg, Russia

^{n} Also at Department of Physics, The University of Michigan, Ann Arbor MI, United States of America

^{o} Also at Louisiana Tech University, Ruston LA, United States of America

^{p} Also at Institucio Catalana de Recerca i Estudis Avancats, ICREA, Barcelona, Spain

^{q} Also at Graduate School of Science, Osaka University, Osaka, Japan

^{r} Also at Department of Physics, National Tsing Hua University, Taiwan

^{s} Also at Department of Physics, The University of Texas at Austin, Austin TX, United States of America

^{t} Also at Institute of Theoretical Physics, Ilia State University, Tbilisi, Georgia

^{u} Also at CERN, Geneva, Switzerland

^{v} Also at Georgian Technical University (GTU),Tbilisi, Georgia

^{w} Also at Ochadai Academic Production, Ochanomizu University, Tokyo, Japan

^{x} Also at Manhattan College, New York NY, United States of America

^{y} Also at Hellenic Open University, Patras, Greece

^{z} Also at Institute of Physics, Academia Sinica, Taipei, Taiwan

^{aa} Also at LAL, Univ. Paris-Sud, CNRS/IN2P3, Université Paris-Saclay, Orsay, France

^{ab} Also at Academia Sinica Grid Computing, Institute of Physics, Academia Sinica, Taipei, Taiwan

^{ac} Also at School of Physics, Shandong University, Shandong, China

^{ad} Also at Moscow Institute of Physics and Technology State University, Dolgoprudny, Russia

^{ae} Also at Section de Physique, Université de Genève, Geneva, Switzerland

^{af} Also at International School for Advanced Studies (SISSA), Trieste, Italy

^{ag} Also at Department of Physics and Astronomy, University of South Carolina, Columbia SC, United States of America

^{ah} Also at School of Physics and Engineering, Sun Yat-sen University, Guangzhou, China

^{ai} Also at Faculty of Physics, M.V.Lomonosov Moscow State University, Moscow, Russia

^{aj} Also at National Research Nuclear University MEPhI, Moscow, Russia

^{ak} Also at Department of Physics, Stanford University, Stanford CA, United States of America

^{al} Also at Institute for Particle and Nuclear Physics, Wigner Research Centre for Physics, Budapest, Hungary

^{am} Also at Flensburg University of Applied Sciences, Flensburg, Germany

^{an} Also at University of Malaya, Department of Physics, Kuala Lumpur, Malaysia

^{ao} Also at CPPM, Aix-Marseille Université and CNRS/IN2P3, Marseille, France

* Deceased